A&A 586, A81 (2016)
DOI: 10.1051/0004-6361/201527326

Astronomy & Astrophysics

High-mass X-ray binaries in the Small Magellanic Cloud⋆

F. Haberl and R. Sturm

Max-Planck-Institut für extraterrestrische Physik, Giessenbachstraße, 85748 Garching, Germany
e-mail: fwh@mpe.mpg.de

Received 8 September 2015 / Accepted 28 October 2015

ABSTRACT

Aims. The last comprehensive catalogue of high-mass X-ray binaries in the Small Magellanic Cloud (SMC) was published about ten years ago. Since then new such systems were discovered, mainly by X-ray observations with *Chandra* and *XMM-Newton*. For the majority of the proposed HMXBs in the SMC no X-ray pulsations were discovered as yet, and unless other properties of the X-ray source and/or the optical counterpart confirm their HMXB nature, they remain only candidate HMXBs.
Methods. From a literature search we collected a catalogue of 148 confirmed and candidate HMXBs in the SMC and investigated their properties to shed light on their real nature. Based on the sample of well-established HMXBs (the pulsars), we investigated which observed properties are most appropriate for a reliable classification. We defined different levels of confidence for a genuine HMXB based on spectral and temporal characteristics of the X-ray sources and colour-magnitude diagrams from the optical to the infrared of their likely counterparts. We also took the uncertainty in the X-ray position into account.
Results. We identify 27 objects that probably are misidentified because they lack an infrared excess of the proposed counterpart. They were mainly X-ray sources with a large positional uncertainty. This is supported by additional information obtained from more recent observations. Our catalogue comprises 121 relatively high-confidence HMXBs (the vast majority with Be companion stars). About half of the objects show X-ray pulsations, while for the rest no pulsations are known as yet. A comparison of the two subsamples suggests that long pulse periods in excess of a few 100 s are expected for the "non-pulsars", which are most likely undetected because of aperiodic variability on similar timescales and insufficiently long X-ray observations. The highest X-ray variability together with the lowest observed minimum fluxes for short-period pulsars indicate that in addition to the eccentricity of the orbit, its inclination against the plane of the Be star circum-stellar disc plays a major role in determining the outburst behaviour.
Conclusions. The large population of HMXBs in the SMC, in particular Be X-ray binaries, provides the largest homogeneous sample of such systems for statistical population studies.

Key words. Magellanic Clouds – galaxies: stellar content – stars: emission-line, Be – stars: neutron – X-rays: binaries – catalogs

1. Introduction

High-mass X-ray binaries (HMXBs) are comprised of an early-type star and a compact object that orbit each other. The compact object is in most cases a neutron star (NS), but it can also be a black hole (see e.g. for the Magellanic Clouds, Liu et al. 2005) or a white dwarf (Sturm et al. 2012, and references therein). Many of the HMXBs show pulsations in their X-ray flux, which indicate the spin period of the NS. The Small Magellanic Cloud (SMC) is peculiar because it hosts exceptionally many known HMXBs. So far, the optical counterpart is only in one (well-confirmed) case a super-giant star (SMC X-1), while for all other identified cases a Be star (with Balmer emission lines) was found, forming a Be/X-ray binary (BeXRB). The last comprehensive catalogue of HMXBs in the SMC was published by Liu et al. (2005). In the meantime, new multi-wavelength data were collected, and many new objects were found with *Chandra*, RXTE, *Swift*, and *XMM-Newton* observations of the SMC, which can at least be treated as candidates for this class of X-ray binaries. Most of the multi-wavelength work on the BeXRBs in the SMC concentrated on these pulsars (Coe & Kirk 2015). In this work we present a complete list of known HMXBs in the SMC, including all sources that have been proposed at least as candidates in the literature. We use multi-wavelength information to identify some of the candidates as likely mis-identifications, and in our final catalogue we devise a scheme according to which the objects are a genuine HMXB system with different confidence levels.

2. Catalogue

For an updated catalogue of HMXBs and candidates in the SMC (and the Magellanic Bridge, which extends beyond the Eastern Wing) we compiled lists from the literature that present properties from large samples or searches for such systems (see Table 1) and include the more recent discoveries of individual objects. We collected information about the X-ray sources as well as their companion stars from the literature and included it in the catalogue to use it for statistical studies. An excerpt of our final catalogue is presented in Table A.1 (first the 63 pulsars sorted according to pulse period, followed by the other objects sorted by coordinates), and the full version is available at the CDS. The content is described in Table 2. In the comment column we provide key references for each source, which are listed in Table A.2.

2.1. Special notes on catalogue sources

The published lists of HMXBs in the SMC disagree in the details for some entries. In particular, sources with uncertain X-ray position or with a pulse period detected with low significance

⋆ The catalogue is only available at the CDS via anonymous ftp to cdsarc.u-strasbg.fr (130.79.128.5) or via http://cdsarc.u-strasbg.fr/viz-bin/qcat?J/A+A/586/A81

Table 1. Literature for HMXBs in the SMC.

Reference	Description
Liu et al. (2005)	HMXB catalogue of the Magellanic Clouds
Coe et al. (2005)	Optical properties of HMXBs in the SMC
Shtykovskiy & Gilfanov (2005)	HMXBs in archival *XMM-Newton* data
McGowan et al. (2008b)	Chandra SMC Wing survey
Galache et al. (2008)	RXTE observations of SMC pulsars
McBride et al. (2008)	Optical spectroscopy of BeXRB pulsars in the SMC
Haberl et al. (2008)	New BeXRBs from *XMM-Newton* observations in 2006 and 2007
Antoniou et al. (2009b)	Optical identification of Chandra sources
Antoniou et al. (2009a)	Optical spectroscopy of BeXRBs in the SMC
Laycock et al. (2010)	Catalogue of SMC sources from deep Chandra observations[a]
Rajoelimanana et al. (2011b)	Long-term optical variability of HMXB pulsars in the SMC
Sturm et al. (2013c)	*XMM-Newton* survey of the SMC
Coe & Kirk (2015)	BeXRB pulsars in the SMC

Notes. [(a)] Includes detections down to two net counts. Most of these low-significance sources are not found in the Chandra Source Catalogue (CSC Evans et al. 2010) .

can lead to different interpretations of their nature. The X-ray position of the majority of sources detected with Chandra or *XMM-Newton* is sufficiently accurate to uniquely identify their optical counterpart. However, there are cases whose angular separation exceeds $2-3\sigma$ confidence, which cause the identification to be uncertain and increase the probability for a chance coincidence of the X-ray source with an early-type star. Moreover, the spin periods of pulsars evolve with time, and detections with an uncertain position of the X-ray source may not be associated uniquely with an object. In the following sections we provide information for such cases to introduce our classifications. In Sect. 2.1.3 we present a list of candidates that were previously rejected as HMXB and that we did not include in the catalogue.

2.1.1. Update on individual BeXRB pulsars

SXP7.92 – A new pulsar with a period of 7.92 s was discovered by (Corbet et al. 2008) in RXTE data. Coe et al. (2009) reported six detections of SXP7.92 with RXTE and suggested AzV285 as the probable optical counterpart. They detected an X-ray source using *Swift* consistently in position with AzV285. Israel et al. (2013) detected 7.92 s pulsations from a source at RA = 00:57:58.4 and Dec = −72:22:29.5 (error 1.5″) in Chandra data. The Chandra source is 20.4′ away from AzV285, but is fully compatible with the RXTE pulsar. The source was probably also detected by ROSAT (RX J0057.9−7222, entry 75 in the HRI catalogue of Sasaki et al. 2000). We conclude that SXP7.92 = CXOU J005758.4−722229 = RX J0057.9−7222 is a BeXRB pulsar and the correct optical counterpart is 2MASS J00575856−7222290. This star shows outbursts every 40.03 days in OGLE II data, which is most likely the orbital period of the binary system (Schmidtke & Cowley 2013). The detection of X-rays from the position of AzV285 with *Swift* suggests that this is the optical counterpart of another BeXRB, which is also confirmed by *XMM-Newton* observations (see below for XMM J010155.7−723236).

SXP9.13 – Pulsations with a period of 9.13 s were discovered from the ASCA source AX J0049−732 (Imanishi et al. 1998). The source is located in a crowded region of the SMC bar with two hard ROSAT sources (RX J0049.5−7310 and RX J0049.2−7311) as possible counterparts (Filipović et al. 2000b). RX J0049.5−7310 was confirmed to be a BeXRB with a spin period of 894 s (Laycock et al. 2010). Consequently, several authors have alloted RX J0049.2−7311 to the 9.13 s pulsar. However, RX J0049.2−7311 was covered by *XMM-Newton* and *Chandra* observations many times with sufficient photon statistics to expect a detection of the 9.13 s period. This was never seen, and therefore we do not identify RX J0049.2−7311 as the 9.13 s pulsar AX J0049−732, but instead keep two separate BeXRBs (within the ASCA error circle of 40″ are ∼25 possible counterparts brighter than $V = 18$ mag with $-0.2 < B - V < 0.2$ in the OGLE BVI photometric catalogue; Udalski et al. 1998).

SXP82.4 – XTE J0052−725 was discovered as a new transient in RXTE data (Corbet et al. 2002), and X-ray pulsations were found in archival Chandra observations. From the RXTE SMC monitoring Galache et al. (2008) identified an outburst pattern with a period of 362.3 ± 4.1 d in X-rays. Rajoelimanana et al. (2011b) analysed the OGLE III data, which revealed a significant peak at 171 ± 0.3 d in the power spectra, which is less than half the reported X-ray period. Galache et al. (2008) already noted that the X-ray period is longer than would be expected given its spin period position in the Corbet diagram (Corbet 1984; Laycock et al. 2005, see also Fig. 8, in which SXP82.4 is found as the right-most open red circle). We add here that the long X-ray period also places XTE J0052-725 outside the relation between $P_{\rm orb}$ and the equivalent width of the Hα line (Reig et al. 1997, see also Fig. 9, in which SXP82.4 is again found as the right-most open red circle). This suggests that the orbital period might be closer to the period found in the optical.

SXP91.1 – Pulsations with ∼91 s were found in RXTE and ASCA data (XTE J0053−724 and AX J0051−722, Corbet et al. 1998). RXTE detections of pulsations at 85.4 s and 89.0 s were initially assigned to individual pulsars, but were later recognised as most likely stemming from one pulsar with a high spin-down rate (Galache et al. 2008; Corbet et al. 2010; Coe et al. 2011a). For our catalogue we only considered one pulsar (SXP91.1).

SXP4693 – The longest period detected from an SMC BeXRB of 4693 s was claimed by Laycock et al. (2010) from a 100 ks *Chandra* observation with ∼140 net source counts. The pulsar was covered by an observation of the *XMM-Newton* survey of the SMC on October 9−10, 2009 (ObsID 0601210801 with a net exposure of about 23 ks and ∼1000 net source counts; Sturm et al. 2013c). A Fourier analysis of the light curve reveals a peak at a frequency consistent with the suggested period. We investigated this further using folding techniques based on χ^2 and Rayleigh Z^2 tests (Buccheri et al. 1983) and a Bayesian periodic signal detection method (Gregory & Loredo 1996) as described for instance in Coe et al. (2012).

Table 2. Catalogue description.

Column	Description
1	Source number
2–3	X-ray coordinates, right ascension and declination (epoch 2000.0)
4	Uncertainty of X-ray position [″]. For *XMM-Newton* positions taken from Sturm et al. (2013c) the 1σ error includes a systematic uncertainty of 0.5″.
5	Origin of the X-ray coordinate (A: ASCA, C: Chandra, E: Einstein, I: Integral, N: *XMM-Newton*, R: ROSAT, S: *Swift*, X: RXTE). When no reliable position could be determined from the non-imaging RXTE collimator-instruments, a radius of 30′ for the position error indicates the size of the field of view.
6	Reference for source discovery.
7	Identification of optical counterpart with emission-line star from Meyssonnier & Azzopardi (1993). The negative number indicates a star found in the catalogue of Murphy & Bessell (2000).
8–15	Flags indicating different source properties. For their description see Table 3.
16	Confidence class (values 1–6, see Table 4).
17–18	Optical coordinates, right ascension and declination (epoch 2000.0) for the identified counterpart from Zaritsky et al. (2002), or – when not available there – from Massey (2002).
19–26	The Magellanic Clouds Photometric Survey (MCPS): U, error(U), B, error(B), V, error(V), I, error(I) [mag] from Zaritsky et al. (2002).
27–32	Colour indices $U-B$, error($U-B$), $B-V$, error($B-V$), $V-I$, error($V-I$) [mag] derived from MCPS photometry.
33–34	Reddening-free Q-value ($Q = U - B - 0.72 \times (B - V)$) and error($Q$) [mag].
35	Near-IR counterpart to the optical star from the Two Micron All Sky Survey (2MASS, Skrutskie et al. 2006).
36–41	Near-IR magnitudes with corresponding errors: J, error(J), H, error(H), K, error(K) [mag].
42–45	Near-IR colour indices, $J-H$, error($J-H$), $H-K$, error($H-K$) [mag].
46–53	Spitzer IRAC fluxes at 3.6, 4.5, 5.8 and 8.0 μm [mag] with respective errors (from the SAGE project, for a description see Meixner et al. 2006).
54	Angular distance between X-ray and optical position [″].
55	Angular distance between optical and near-IR position [″].
56	Neutron star spin period [s] inferred from X-rays.
57	Orbital period [days] (see flags for origin).
58–59	Maximum and minimum X-ray flux [erg cm^{-2} s^{-1}] when available in the 0.2–10 keV band. Fluxes in the SMC *XMM-Newton* catalogue of Sturm et al. (2013c) are given for the 0.2 to 4.5 keV band. To convert them into the 0.2–10 keV band, we multiplied them by a factor of 2.6 assuming a standard power law with photon index 0.9 (Haberl et al. 2008) and a column density of 10^{21} cm^{-2} (solar abundance). For *Swift* XRT count rates we used a flux conversion factor of 1.1×10^{-10} erg cm^{-2} cts^{-1}
60	Flag for minimum flux: 1 for a non-detection with an upper limit; −1 when unknown; 0 for detection.
61–62	References for maximum and minimum X-ray flux.
63	X-ray variability factor (ratio of maximum to minimum flux).
64	Equivalent width of the Hα line [Å] (minimum value if more than one measurement is available).
65	Maximum equivalent width of the Hα line [Å].
66	References for the Hα measurements.
67	Comments with key references.

This resulted in a formal pulse period with 1σ uncertainty of 4700 ± 150 s (see Fig. 1). The light curve (Fig. 2) shows dips, which repeat every ∼4800 s; they are most likely responsible for the periodicity seen in the timing analysis. To confirm that this pattern is strictly periodic requires a longer observation, but we conclude that the *XMM-Newton* observation finds evidence for a period around 4800 s in agreement with the *Chandra* results presented by Laycock et al. (2010). Coe & Kirk (2015) listed the pulsar twice with two different periods as SXP6.62 and SXP4693. We do not see a significant signal near 6.62 s in the *XMM-Newton* data.

2.1.2. Sources without detected pulsations

RX J0032.9−7348 – This hard and variable ROSAT source was discovered by Kahabka & Pietsch (1996) in PSPC observations and proposed as HMXB candidate. Stevens et al. (1999) found two early-type stars in the ROSAT error circle, one of them showing Hα emission (their object 1). Object 2 was identified with GSC0914101338, for which (Evans et al. 2004) give a spectral type of B0.5V. Object 2 is brighter (B = 15.50 mag, V = 15.24) and slightly more distant to the best PSPC position (Haberl & Sasaki 2000). Although object 2 cannot be completely ruled out, we assume object 1 as optical counterpart of the X-ray source because of its measured Hα emission line, which suggests a BeXRB nature, but we flag the optical identification as uncertain.

RX J0045.6-7313 – Haberl & Sasaki (2000) suggested this ROSAT source as a BeXRB candidate because an emission-line star is located in the X-ray error circle (object 114 in Meyssonnier & Azzopardi 1993). More recent catalogues of early-type stars in the SMC contain additional possible counterpart candidates: Bonanos et al. (2010) performed IR photometry of massive stars and listed AzV9 (Azzopardi et al. 1975) with spectral class B0III (UV spectral classification by Smith Neubig & Bruhweiler 1997) and IR colours consistent with that of a Be star (see Sect. 3 and Fig. 4). We add AzV9 to our catalogue and flag the optical identification as uncertain.

CXOU J004941.43−724843.8 – This source was detected in the Chandra survey of the SMC bar (Antoniou et al. 2009b, source ID 7_19) with the proposed optical counterpart (V = 17.17 mag) 1.36″ away from the X-ray position. With an X-ray luminosity of 3.7×10^{33} erg s^{-1} the source was at low luminosity during the Chandra observation (Maravelias et al. 2014), and it was not detected by *XMM-Newton* (Sturm et al. 2013c). Maravelias et al. (2014) presented spectroscopy of the optical star and reported the detection of a narrow Hα line, concluding on a spectral type B1-B5 but uncertain Be nature because

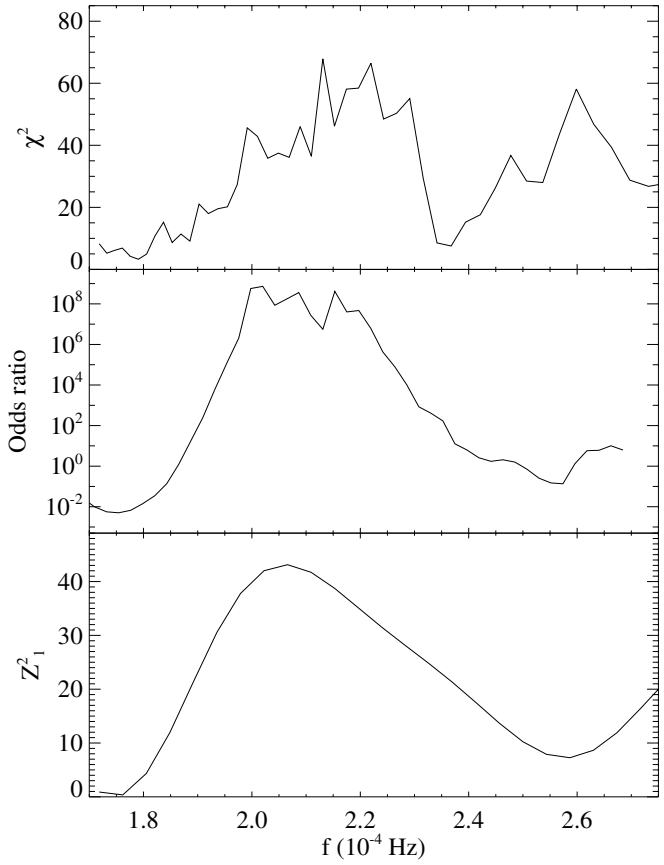

Fig. 1. Periodograms obtained from the combined EPIC data of SXP4693 from the *XMM-Newton* observation 0601210801 (0.2−10 keV). χ^2 test, Bayesian odds ratio, and Rayleigh Z^2_1 test are shown *from top to bottom*.

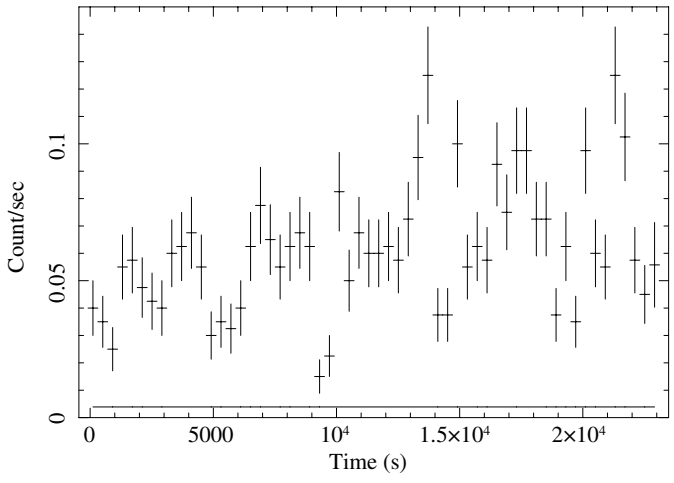

Fig. 2. EPIC light curve (0.2−10 keV) of SXP4963 with a binning of 400 s. The horizontal line at 3.9×10^{-3} cts s^{-1} marks the background level.

of the marginal line width. All these ambiguities make this case inconclusive.

XMMU J005723.4−722356 – Shtykovskiy & Gilfanov (2005) proposed the source detected in *XMM-Newton* data as an HMXB candidate because it might be associated with an early-type star. The spectral type of the proposed counterpart was given as B2 (II) by Evans et al. (2004) and confirmed by Maravelias et al. (2014). In the SMC catalogue (source 65) of Sturm et al. (2013c), the *XMM-Newton* position is 1.73″ offset from the optical position given by Zaritsky et al. (2002). Similarly, the Chandra position is 1.3″ away (Antoniou et al. 2009b; Maravelias et al. 2014). Both X-ray positions are more consistent with that of an AGN (Sturm et al. 2013c). The source was also detected in three recent *XMM-Newton* observations of SXP5.05 (Coe et al. 2015) at a much brighter level than in the past. During the last observation (ID 0700580601) in particular, with 2.4 $\times 10^{-13}$ erg cm^{-2} s^{-1} the flux was a factor of ∼5 higher than the previous maximum during observation 0084200101. Using the upper limit from observation 0500980201 of 5.8 $\times 10^{-15}$ erg cm^{-2} s^{-1}, we derive a variability factor of at least ∼40, which strongly favours an HMXB. The X-ray position in all three new observations also agrees better with the B2 star (distances between 0.45″ and 1.0″), which is further improved when using the target of the observations, SXP5.05 and its optical counterpart, for bore-sight corrections (resulting in distances of between 0.36″ and 0.68″). Optical identification with the early-type star and the strong X-ray variability suggest that XMMU J005723.4−722356 is an HMXB.

XMM J010155.7−723236 – Source number 816 in the SMC catalogue of Sturm et al. (2013c) was originally assigned to SXP7.92. However, no pulsations were detected in the *XMM-Newton* data. The improved *XMM-Newton* position is consistent with the *Swift* source detected near AzV285 (see SXP7.92 above) and confirms this star as the optical counterpart. A flux upper limit from one *XMM-Newton* observation with no detection of the source combined with the *Swift* flux yields a flux ratio of >900, clearly suggesting a BeXRB nature of the source. Analysing OGLE II and III data of AzV285, (Coe et al. 2009) found a 36.79 d period, which was revised by Rajoelimanana et al. (2011b) to 36.41 ± 0.02 d; this is probably the binary period.

XMMU J010429.4−723136 – Source number 3285 in the SMC catalogue of Sturm et al. (2013c) was proposed by these authors as an HMXB candidate. The large X-ray variability and the brightness of the proposed optical counterpart indicates a BeXRB nature of the source. The source is most likely identical to the Chandra source CXOU J010428.7−723134 (Rajoelimanana et al. 2011a; Schmidtke et al. 2013a), although the Chandra position is 2.8″ away from that of the proposed counterpart (using the coordinates from Zaritsky et al. 2002). The optical star shows a period of 37.15 days in OGLE and MACHO data (Rajoelimanana et al. 2011a), which might indicate the orbital period, but could also be an alias of a 0.972 d period, which Schmidtke et al. (2013a) interpreted as non-radial pulsations of a Be star. Rajoelimanana et al. (2011a) also reported a period of 707 s found in the Chandra X-ray data. However, this period is most likely an instrumental effect: it is exactly the Chandra dithering period and the source is located at the rim of a CCD, moving in and out of the detector. This probably also explains the relatively large angular distance between the Chandra and the optical position. A likely ROSAT detection ([HFP2000]264) is listed in the PSPC catalogue of Haberl et al. (2000). We conclude that XMMU J010429.4−723136 = CXOU J010428.7−723134 = RX J0104.5−7231 is a BeXRB in the SMC, although measurements of the spin period of the NS and of the strength of the Hα line are still required for the final confirmation.

2.1.3. Rejected candidates from previous work

For completeness we provide here a list of former HMXB candidates, which were rejected in earlier work. These objects are not included in our catalogue.

XMMU J004833.4−732355 – Source number 40 (uncertain nature) in Table 2 of Shtykovskiy & Gilfanov (2005) is classified as an AGN by Sturm et al. (2013c). See source 123 in their catalogue.

XMMU J005156.0−734151 = RXJ0051.7−7341 – Source number 1 of Sasaki et al. (2003) is rejected as an HMXB candidate. In the improved error circle of the source derived from additional observations (source 100 in the SMC catalogue of Sturm et al. 2013c) no bright optical counterpart with colours of an early-type star is found.

XMMU J005432.2−721809 – Source number 36 (uncertain nature) in Table 2 of Shtykovskiy & Gilfanov (2005) is newly classified as AGN (source 62 in Sturm et al. 2013c). From the X-ray spectrum a photon index typical for an AGN is derived and the position is 2.7″ (4.8σ) away from the V = 16.6 mag star, originally proposed as the counterpart.

XMMU J005441.1−721720 – Another source of uncertain nature (number 41) from Shtykovskiy & Gilfanov (2005). The revised position (source 82 in Sturm et al. 2013c) is inconsistent with the originally proposed counterpart (V = 15.7 mag star), and the source is classified as AGN candidate.

CXOU J005504.40−722230.4 – Maravelias et al. (2014) presented optical spectroscopy of a B star 3.6″ away from the Chandra position. The large angular distance and the faintness (V = 17.86 mag) of this star make a misidentification very likely. Moreover, from the *XMM-Newton* detection of the X-ray source (source 976 in Sturm et al. 2013c) the most likely counterpart is classified as AGN using a mid-IR colour selection (Kozłowski & Kochanek 2009).

CXOU J005527.9−721058 was found in Chandra data and suggested as a BeXRB pulsar by Edge et al. (2004b,a). The source was later detected by *XMM-Newton* (XMMU J005527.6−721059). The two X-ray positions obtained from Chandra and *XMM-Newton* are inconsistent with that of the proposed Be star counterpart. Furthermore, the X-ray spectrum is more typical of an AGN, making it highly likely that the period, detected with only 2.5σ confidence, was spurious and the identification with the Be star was incorrect (Haberl & Eger 2008).

XMMU J010016.1−720445 = RX J0100.2−7204 – Additional *XMM-Newton* observations of source number 11 of Sasaki et al. (2003) provide an improved position that excludes identification with a bright optical counterpart. The X-ray source is classified as an AGN candidate (source 55 in Sturm et al. 2013c).

XMMU J010137.4−720418 = RX J0101.6−7204 – This source is located close to the *XMM-Newton* calibration target 1E 0102.2−7219 and was detected more than 30 times. The error-weighted X-ray position is incompatible with that of the emission-line star [MA93]1277 (Meyssonnier & Azzopardi 1993), which was proposed by Sasaki et al. (2000) as possible counterpart in a BeXRB. The source appears as entry 21 in Shtykovskiy & Gilfanov (2005). The steepness of the power-law X-ray spectrum and the small X-ray variability of a factor of ∼4 over 12 yr of *XMM-Newton* observations are fully compatible with an AGN nature (source 53 in Sturm et al. 2013c).

AX J0105−722 – The detection of a 3.34 s periodicity with 99.5% confidence (2.8σ) was claimed by Yokogawa & Koyama (1998b). The X-ray spectrum was modelled with a power law with photon index 2.2 ± 0.3, which is much steeper than typically found for HMXBs in the 0.2−10 keV band. RX J0105.1−7211 was suggested as the most likely ROSAT counterpart of the ASCA source with MA93[1517] (Meyssonnier & Azzopardi 1993) located 7.7″ away from the ROSAT position (Filipović et al. 2000a). Another nearby emission line star (MA93[1506]) was identified as Be star of spectral type B1-B2 III–Ve (with equivalent width of the Hα line of −54 Å) and favoured as counterpart because it has an optical period of 11.09 d (Coe et al. 2005; McBride et al. 2008). However, such a short orbital period is not expected from the Hα – orbital period relation, which suggests on orbital period longer than 100 d (Fig. 9). Eger & Haberl (2008a) used *XMM-Newton* observations to improve the X-ray position and classified XMMU J010509.7−721146 (power-law photon index 2.0 ± 0.3; no V < 18 optical counterpart in error circle) as AGN. Positional coincidence and the agreement in X-ray spectral properties strongly suggest that AX J0105−722, RX J0105.1−7211 and XMMU J010509.7−721146 are the same source and incompatible with [MA93] 1517 and [MA93] 1506 as optical counterpart. The 3.34 s periodicity is most likely spurious (but still appears in the list of Coe & Kirk 2015).

XMMU J010519.9−724943 – As optical counterpart, Maravelias et al. (2014) suggested a B3-B5 star with Hα emission 4.0″ from the X-ray position determined by these authors. Based on astrometric corrections and combining data from two *XMM-Newton* observations, Sturm et al. (2013c) derived a position 4.9″ away from the optical position (source 420 in the *XMM-Newton* catalogue). This corresponds to 5σ, making the identification highly unlikely. Given the classification as AGN by Sturm et al. (2013c), we conclude that the Be star is not the counterpart of the X-ray source.

XMMU J010620.0−724049 – This case is very similar to the previous, here the separation Chandra/optical position is 4.5″. Again *XMM-Newton* detections in two observations provide an X-ray position (source 426 in *XMM-Newton* SMC catalogue) that is even farther away (7.6″). A very likely AGN-counterpart is detected in *Spitzer*/IRAC images[1] located only 0.64″ from the *XMM-Newton* position. We conclude that the X-ray source is not a BeXRB, but an AGN.

3. Confidence classes of HMXBs and candidates

Candidates for HMXBs in the SMC were proposed in various publications mainly based on the positional coincidence of an X-ray source with an optical counterpart with appropriate brightness and colours consistent with an early-type star. The confidence with which they can be claimed to be a real HMXB or a BeXRB depends in particular on various aspects, such as the error of the X-ray position (usually significantly larger than the uncertainty in the optical position) and properties of the X-ray source as well as the candidate optical counterpart. This includes spectral and timing properties of the X-ray source and the optical star. When several criteria can be applied successfully, the confidence increases for a correct association of the X-ray source and the optical counterpart and its identification as an HMXB. Following this, we assigned flags to the (candidate) HMXBs in our compiled catalogue as described in Table 3.

Based on the flags, we divided the list of HMXBs and candidates into six confidence classes, which are summarised in Table 4. Sources with detected pulse period in X-rays (class I with flag ps or ps:) are most likely HMXBs even when the optical counterpart is not clearly identified as yet because the uncertainties in the X-ray position are large. X-ray sources with large long-term variability or a hard spectrum as typical for BeXRBs (in the 0.2−10 keV band the photon index is lower than ∼1.3;

[1] SAGE LMC and SMC IRAC Source Catalog (IPAC 2009) available in Vizier.

Table 3. Flags indicating different properties as measured for HMXBs and candidates.

C[a]	Flag[b]	Description
8	ps	X-ray modulation indicates NS spin period
9	px	long-term X-ray period suggests orbital period
10	po	period in optical suggests orbital period
11	os	orbital solution available
11	ox	assuming X-ray period as orbital period
11	oo	assuming optical period as orbital period
11	oxo	X-ray and optical period are consistent
12	xv	variability in X-rays larger than a factor 30
13	xs	typical X-ray spectrum (power law with photon index <1.3)
14	oi	optical id with high confidence
15	em	Balmer (Hα) emission measured from spectrum
15	nem	no near-IR excess emission

Notes. [(a)] Column in catalogue table (see Table 2). [(b)] A colon behind the flag indicates an uncertain property.

Table 4. Summary of confidence classes.

Class	Flags	Number of sources
I	ps ∪ ps:	63
II	xv ∪ xs	18
III	oi ∩ em	12
IV	oi: ∩ em	8
V	oi	3
VI	oi:	44

Haberl et al. 2008) can also be identified as HMXBs from their X-ray properties (class II with flag xv or xs). A third class with secure identification of the optical counterpart (due to a precise X-ray position) as an early-type emission-line star (flags oi and em) are also BeXRBs with high confidence. With increasing uncertainty in the X-ray position, the chance coincidence for the presence of an early-type star in the error circle increases. A larger X-ray position error is typically found for weak X-ray sources, which do not allow deriving other X-ray properties either. In class IV we list X-ray sources with less certain position and an emission-line star in the error circle (flags oi: and em). Class V comprises X-ray sources with a good position and therefore high confidence for their identification with early-type stars (flag oi). However, no information about Hα emission is available. Only three such sources are found in our catalogue, and optical spectra should easily allow confirming their probable Be-star counterpart. Finally, in class VI the highest fraction of chance correlations of the X-ray sources with early-type stars is expected. These are usually weak X-ray sources (flag oi: with position errors typically larger than 1″), and apart from the appropriate colours, no other information about the possible optical counterpart is available.

As mentioned above, the probability for false identification of optical counterparts to the X-ray sources in class VI is higher than for classes I–V. The optical counterparts of the large majority of the BeXRB pulsars in class I are well investigated. Spectral types and the strength of the Hα emission were determined and can be found in the literature (e.g. Coe et al. 2005; McBride et al. 2008). Therefore, class I objects can be used to define a representative sample. Comparison of various source parameters between the different classes may then reveal differences, which indicate false identifications.

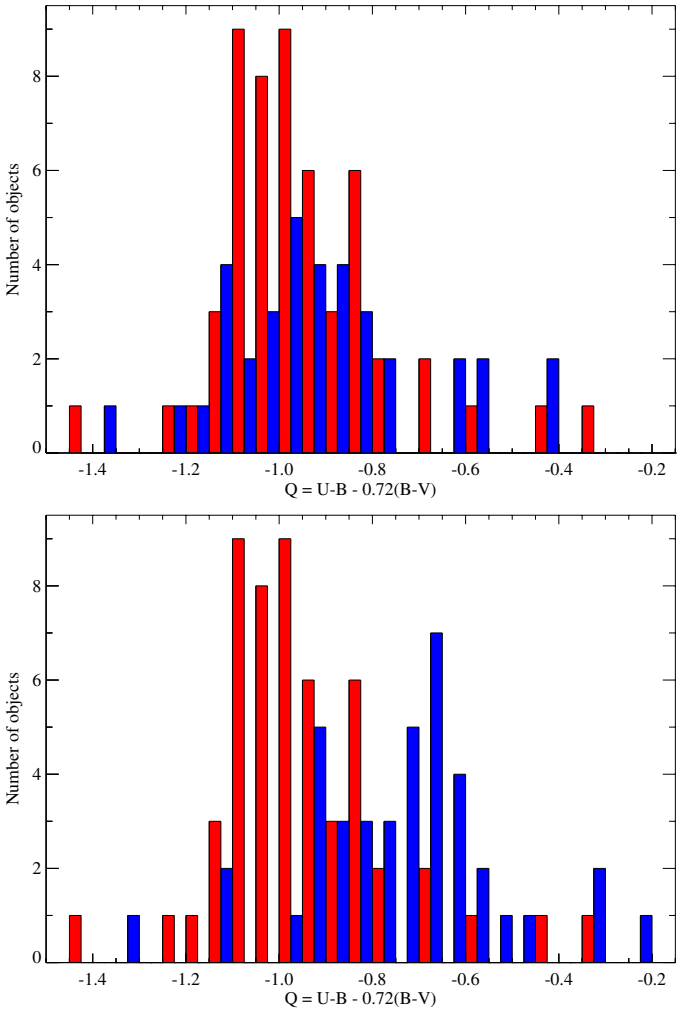

Fig. 3. Distribution of the reddening-free Q parameter for different HMXB confidence classes. The top panel compares the pulsars (class I) with identified optical counterpart (red) with objects from classes II to V (blue), while in the bottom panel the comparison with class VI is shown.

When we plotted colour-colour ($U-B$ vs. $B-V$) and colour-magnitude (V vs. $B-V$) diagrams, we found evidence that the objects in class VI are optically fainter and redder. To make this quantitatively clearer, we used the reddening-free Q-factor $Q = U - B - 0.72(B-V)$ and compared its distribution between the different classes. While classes II–V are statistically consistent with class I, class VI exhibits a significantly different distribution towards higher Q values. This is demonstrated in Fig. 3 where the distribution of the Q parameter is compared for class I and class II–V (top panel) and for class I and class VI (bottom). A statistical Kolmogorov-Smirnov test results in a probability of 98.5% for class I and II–V and 1.3×10^{-7} for class I and VI to be drawn from the same distribution. This clearly shows that the early-type stars proposed as optical counterparts of the X-ray sources from class VI are on average of different (later) spectral type than the optical counterparts of class I, which show a relatively narrow distribution around B0-B1 (McBride et al. 2008). In particular, no spectral type later than B2 was found for BeXRBs with well-known optical counterpart in the Milky Way (Reig 2011). On the other hand, isolated Be stars with later spectral type exist (McBride et al. 2008), and we cannot exclude that (in particular X-ray faint) class VI objects might be associated with a late-type BeXRB. However, the larger X-ray error

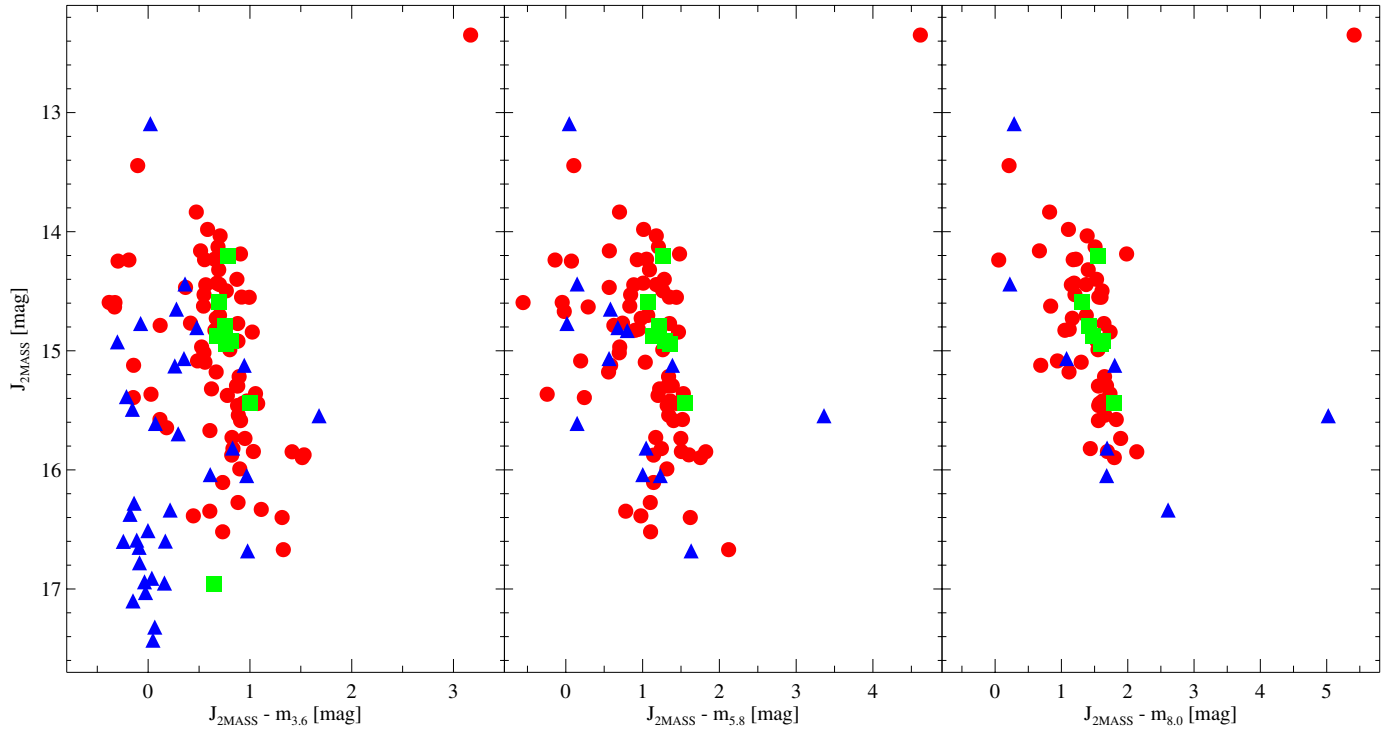

Fig. 4. Infrared excess using the three IRAC magnitudes at 3.6, 5.8, and 8.0 μm and J band from 2MASS (in a few cases from IRSF when no 2MASS value was available). Blue triangles mark sources from class VI (flag "oi:"), green squares those from class IV (with additional flag "em"), while red circles indicate flag "oi".

circles of the faint class VI objects implies that many of them are chance coincidences of the X-ray sources with single late B- or even Be-type stars.

Bonanos et al. (2010) have used Spitzer IRAC fluxes (at 3.6, 4.5, 5.8, and 8.0 μm) of O and early-B stars in the SMC to distinguish OBe from OB stars based on their infrared excess relative to J-band fluxes. In Fig. 4 we plot the infrared excess for the catalogue sources with flags "oi" and "oi:". A remarkably large portion of sources from class VI (16 out of 44) fall in a region with $J > 16$ and $J - m_{3.6} < 0.3$ where no other sources are found. This suggests that these 16 objects are most likely normal B stars without a circum-stellar disc (Bonanos et al. 2010, where a threshold of $J-m_{3.6} > 0.5$ is defined to introduce a photometric Be star classification). Fourteen of the sixteen objects are from the BeXRB candidate list derived from the *XMM-Newton* survey of the SMC (sources 41, 259, 468, 474, 1019, 1189, 1762, 1955, 2211, 2569, 2675, 2721, and 2967, 3271 from Sturm et al. 2013c). The authors determined the number of chance coincidences as high as twenty. Therefore, the lack of infrared excess excludes the greater part of the expected chance coincidences. The remaining two objects (CXO J005331.8-721845 and CXO J005419.2-722049) are from the candidate list of Laycock et al. (2010), very faint X-ray sources with positional errors larger than 5″. Neither are found in the CSC. The proposed optical counterparts have optical colours consistent with an early-type star. They do not show infrared excess, which suggests that they are not Be stars and therefore are most unlikely the counterparts of the weak Chandra sources, which might even be spurious detections after all. This is also supported by their Q-values, which are >-0.91. We flag these sixteen objects with "nem" in the catalogue.

As expected, the class IV objects are among the well-established BeXRBs, as is shown by their flag "em". However, it should be noted that for class IV objects a misidentification of the X-ray source with a Be star can still not be excluded: as a result of their larger X-ray position uncertainty, the number of chance coincidences is higher than for objects whose optical counterpart is unambiguously identified (flag "oi").

4. Candidates that are probably misidentified as HMXBs

In Sect. 3 we have shown that a large portion of the 44 sources in confidence class VI is most likely misidentified as HMXBs. New data for some of the proposed candidates further contradict their proposed HMXB nature. In the following we list objects that we finally consider to probably not be HMXBs or which we reject.

Sturm et al. (2013c) present a list of 45 HMXB candidates selected from their SMC X-ray source catalogue (see their Table 5). Taking into account the positional uncertainties of the X-ray sources, they estimate 16.6 ± 3.4 chance coincidences. Meanwhile, additional information is available for many of the candidates, which allows us to better constrain the origin of their X-ray emission. This includes Chandra X-ray data (with source positions often available from the on-line catalogue of Evans et al. 2010), possible AGN counterparts properly selected from Spitzer data using colour indices (SAGE LMC and SMC IRAC Source Catalog – IPAC 2009), and absence of a near-IR excess, normally seen from Be stars (see Sect. 3). In particular, McBride et al. (2016) have obtained optical spectroscopy of all candidates presented by Sturm et al. (2013c), and in several cases no Balmer emission was found (although Hα was not always covered). It should be noted here that Be stars can lose and rebuild their circum-stellar disc, as is indicated by the disc emission coming and going on timescales of decades (Rivinius et al. 2013) with

state transitions as short as a few months (e.g. Reig et al. 2007). Although we consider a disc loss between X-ray and optical observations unlikely, we cannot exclude that a BeXRB is observed during a disc-less state. Therefore, we label cases without an indication of a circum-stellar disc because there is no near-IR excess *or* Balmer emission as "HMXB unlikely" and only cases without near-IR excess *and* no Balmer emission as "HMXB rejected" in the comment column of the catalogue. We kept the unlikely/rejected cases in our catalogue. We also rejected candidates with improved X-ray positions that exclude the previously suggested counterparts, candidates that are more probably AGN because of their Spitzer counterparts and other information (summarised below).

At the current status of our work, this means that we have 27 candidates in total (11 marked as unlikely and 16 as rejected) that probably are HMXB misidentifications. Twenty-five of them belong to confidence class VI, only one was given class III ([SHP2013] 1408, see below) and one class V ([SHP2013] 287, see below). Twenty of the twenty-seven sources are from the candidate list of Sturm et al. (2013c). From this list we can confirm fourteen sources as HMXBs, and for eleven cases no additional information is available and they remain candidates. Following SIMBAD naming conventions, we use [SHP2013] N for source number N in the catalogue of Sturm et al. (2013c) and [SG2005] SMC N for sources in Table 2 of Shtykovskiy & Gilfanov (2005).

For [SHP2013] 117 = [SG2005] SMC 34 a V = 16.2 mag star was proposed as the optical counterpart. Sturm et al. (2013a) argued for QSO J004818.72-732059.83 (Kozłowski & Kochanek 2009) as another likely counterpart, very close to the X-ray position. McBride et al. (2016) found no Balmer emission from the early-type star, making the QSO the more likely counterpart.

A V = 16.7 mag star (with spectral type B2 V Nazé et al. 2003b) was proposed as counterpart for [SHP2013] 160 = [SG2005] SMC 39. No Balmer emission McBride et al. (2016) and the presence of a Spitzer counterpart make an AGN nature more likely.

[SHP2013] 259 = [SG2005] SMC 48 was identified as an eclipsing binary with an orbital period of 5.18 days (Wyrzykowski et al. 2004). This makes an HMXB nature highly unlikely.

A V = 15.1 mag star (with spectral type B1-3 III from the 2dF survey of the SMC, Evans et al. 2004) was proposed as the counterpart for [SHP2013] 287. McBride et al. (2016) found no Balmer emission from the early-type star, suggesting a chance coincidence with the X-ray source.

The proposed counterpart of [SHP2013] 474 shows no near-IR excess (see Sect. 3), and McBride et al. (2016) found no Balmer emission.

For [SHP2013] 562 a V = 15.4 mag star with spectral type B0 V from the 2dF survey (Evans et al. 2004) was proposed as counterpart. McBride et al. (2016) found no Balmer emission.

The angular distance between [SHP2013] 1019 and its proposed optical counterpart is 3.5″. McBride et al. (2016) found no Balmer emission. No near-IR excess is seen either (see Sect. 3). The presence of a Spitzer counterpart makes a chance coincidence with the early-type star most likely and suggests an AGN origin for the X-ray source.

[SHP2013] 1189 is located about 3.5′ from 1E0102.2-7219, the X-ray brightest supernova remnant in the SMC that is frequently observed by *XMM-Newton*. The faint source was detected only once with a large positional error, and no entry is found in the Chandra on-line catalogue near its position. However, the source is clearly seen in the merged Chandra ACIS-I image presented in Sturm et al. (2013c), which suggests a constantly faint source. The Chandra position is incompatible with that of the V = 16.1 mag star proposed as counterpart. This star also shows no near-IR excess.

[SHP2013] 1408 is associated with the B[e] super-giant star LHA 115-S 18 (Clark et al. 2013; Maravelias et al. 2014), and the X-ray emission is probably not produced by accretion onto a compact object.

The case of [SHP2013] 1762 is very similar to [SHP2013] 1189: near 1E0102.2-7219; seen in the merged Chandra ACIS-I image; Chandra position incompatible with the V = 16.3 mag star proposed as counterpart, which shows no near-IR excess.

McBride et al. (2016) identified the proposed counterpart to [SHP2013] 1823 as Be star. However, the uncertain *XMM-Newton* position is at a distance of 4.9″. The source was also detected in Chandra data (Laycock et al. 2010), also 5″ from the optical position. The Chandra 95% uncertainty of 1.83″ makes the identification of the X-ray source with the Be highly unlikely. Moreover, the existence of a Spitzer counterpart suggests an AGN origin.

The *XMM-Newton* detection of the weak source [SHP2013] 1826 yields a highly uncertain position and is 5.7″ away from its proposed optical counterpart. In addition, a Chandra detection (95% error = 0.47″, distance 5.4″ Laycock et al. 2010) excludes an identification with the proposed V = 14.9 mag star.

The proposed counterpart of [SHP2013] 1955 shows no near-IR excess (Sect. 3), and McBride et al. (2016) found no Balmer emission. We conclude that the X-ray source is not associated with the normal B star.

The angular distance between [SHP2013] 2100 and its proposed optical counterpart is 4.3″, and McBride et al. (2016) found no Balmer emission.

The position of the proposed counterpart of [SHP2013] 2318 is 5.7″ away. We determined an improved position from a recent deep Chandra observation (ID 14671) to an accuracy of 0.3″ (1σ). The Chandra position is within 2.0″ of the *XMM-Newton* position, but with 6.9″ distance incompatible with that of the V = 16.1 mag early-type star.

McBride et al. (2016) found no Balmer emission from the suggested counterpart of [SHP2013] 2497, which makes a chance correlation with a normal B star most likely.

No near-IR excess and no Balmer emission are seen from the suggested counterpart of [SHP2013] 2569 McBride et al. (2016). The existence of a Spitzer counterpart suggests an AGN origin.

[SHP2013] 2675 is another case that was identified as an eclipsing binary (orbital period of 3.29 days Wyrzykowski et al. 2004), which makes an HMXB nature highly unlikely. No near-IR excess is seen from the binary star system.

For [SHP2013] 2737 a V = 14.7 mag star with spectral type B5 II from the 2dF survey (Evans et al. 2004) was proposed as counterpart. McBride et al. (2016) found no Balmer emission. A Chandra detection (Evans et al. 2010) yields a position 2.9″ from the B star. A Spitzer counterpart suggests an AGN origin.

The V = 16.6 mag star suggested as counterpart for [SHP2013] 3271 is 4.4″ away from the *XMM-Newton* position. McBride et al. (2016) found no Hα emission. No detected near-IR excess is consistent with a normal B star found by chance in the X-ray error circle.

5. Population statistics

The large number of HMXBs in the SMC allows statistical investigations of their X-ray and optical properties. Many BeXRBs were found because coherent pulsations in the X-ray flux (often during outburst) were detected, which indicates the spin period of the NS. Knigge et al. (2011) discussed the bimodal distribution of the spin period with two maxima at around 10 s and between 100 s to 1000 s in terms of two populations of X-ray pulsars produced by two types of supernovae. As an alternative explanation, Cheng et al. (2014) proposed that the spin period distribution is the result of two different accretion modes. To elaborate on this question, we collected maximum and minimum fluxes (or upper limits when lower) reported for the SMC BeXRBs in the literature and entered them in our catalogue. The high sensitivity of the *XMM-Newton* SMC survey provides stringent upper limits for non-detected sources. These are available in the catalogue of Sturm et al. (2013c) for sources observed more than once and detected at least once. For the remaining SMC HMXBs, which were never detected in any *XMM-Newton* observation, we readout the upper limits from the sensitivity maps produced for the work of Sturm et al. (2013c). If an *XMM-Newton* upper limit was higher than any detected (minimum) flux from another instrument, then it was not used. In Fig. 5 we plot the maximum and minimum fluxes ($F_{\rm max}$ and $F_{\rm min}$) and the derived ratio (variability factor) for the SMC BeXRB pulsars versus their spin period. As shown by Cheng et al. (2014), short-period (<40 s) pulsars show on average higher maximum luminosities than long-period pulsars. This is demonstrated by the rather loose anti-correlation of maximum flux with spin period in the upper panel of Fig. 5. We note that the minimum observed flux (or upper limit for non-detections) also tends to be lower for the short-period pulsars. While most of the short-period pulsars even fall below the detection limits of modern X-ray instrumentation, many long-period pulsars are always detected well above these limits (Fig. 5, middle panel). As a consequence, the anti-correlation of $F_{\rm max}/F_{\rm min}$ with spin period is even more pronounced (Fig. 5, lower panel). There still might be some observational bias in the correlations, since some systems have not been caught at outburst maximum or at their minimum flux level and the observed $F_{\rm max}/F_{\rm min}$ value presents only a lower limit. However, given the large number of X-ray observations, this should affect only a relatively small number of objects independent of spin period and would not change the overall distributions. It is therefore remarkable that the upper envelope of the data points in the bottom panel of Fig. 5 is so sharp, suggesting that the neutron stars with longer spin periods – and wider orbits (Fig. 8) – sample a narrower range in accretion rate than short-period pulsars. The largest variations in accretion rate are expected for systems with high eccentricity and/or large tilt between orbital plane and Be disc.

For six of SMC XRBs the eccentricity of the orbit is known with values between 0.07 and 0.43. Interestingly, among these, SMC X-2 has the lowest eccentricity and the highest variability factor of $\sim 5 \times 10^4$. Although the orbital parameters could be determined only for neutron stars with short spin periods (which show the highest variability), the measured eccentricities are relatively moderate. This may indicate that eccentricity is not the main parameter leading to the strong outbursts from these systems. Alternatively, a considerable inclination of the orbit with respect to the plane of the circum-stellar disk can also lead to strong and in particular short outbursts when the NS passes through the disc. Strong evidence for this kind of system geometry was found for SXP5.05 (Coe et al. 2015). A high inclination with the NS moving far above and below the disc can also explain the lower minimum X-ray flux values observed from systems with short spin period (and high variability). Moreover, such a system geometry is thought to cause a strong warping of the disc, which then can lead to the strong X-ray outbursts and high spin-up of the NS to short periods (Cheng et al. 2014).

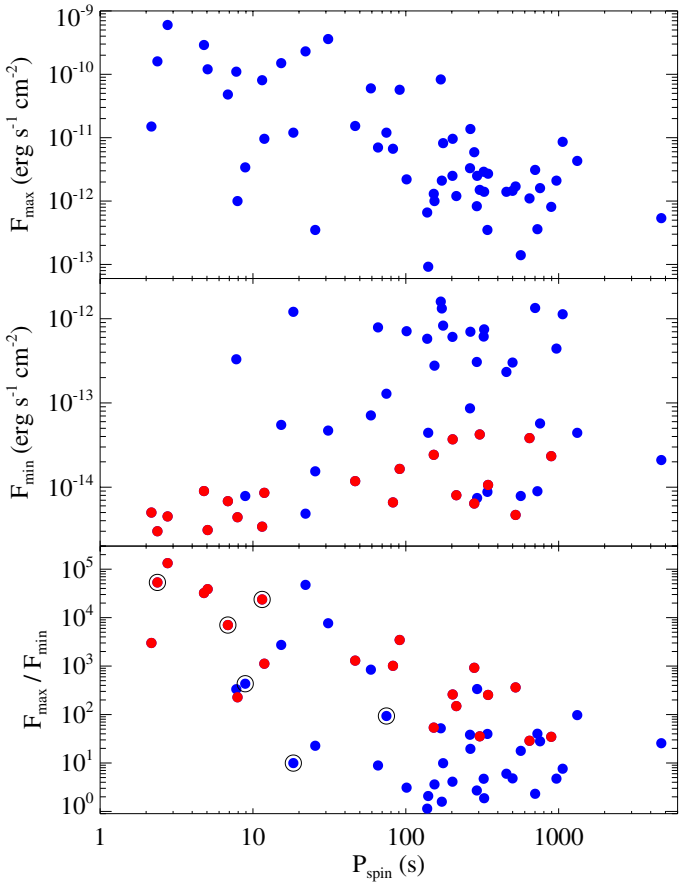

Fig. 5. Observed maximum (*top*) and minimum (*middle*) X-ray flux together with their ratio (*bottom*) as function of spin period. When sources were not detected in a second observation, available upper limits were used for the minimum flux (marked in red). Black circles in the bottom panel indicate the BeXRBs with measured orbit eccentricity.

While maximum fluxes seen from BeXRBs are mainly determined by the available supply of matter along the neutron star orbit, the observed minimum flux is very likely influenced by another mechanism. The propeller effect can inhibit accretion when the matter from the accretion disc couples onto the rotating magnetosphere of the neutron star at distances larger than the co-rotation radius (Stella et al. 1986). The critical luminosity strongly depends on the spin period (Eq. (5) of that paper) and is expected to be about 2.7×10^{36} erg s^{-1} for instance for SMC X-2 with a period of 2.37 s. The large variability factors of short-period pulsars might be explained by this mechanism. When magnetospheric accretion stops, only faint emission from the (cooling) neutron star surface remains, possibly with some small contribution from direct accretion. Several BeXRB pulsars observed in extreme low states at X-ray luminosities of $\sim 10^{34}$ erg s^{-1} and below are believed to be seen in the propeller state (see Raguzova & Popov 2005, and references therein). For long-period pulsars the propeller effect is thought to play no role (e.g. for a period of 400 s the critical luminosity is at 1.7×10^{31} erg s^{-1}). However, we note

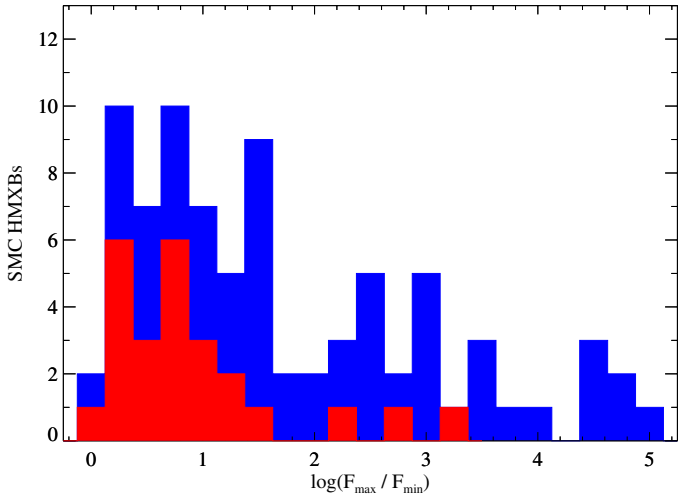

Fig. 6. Distribution of the variability factor F_{max}/F_{min} for all HMXBs with confidence class I–V (blue) and for the non-pulsars (confidence class II–V, red) in the SMC.

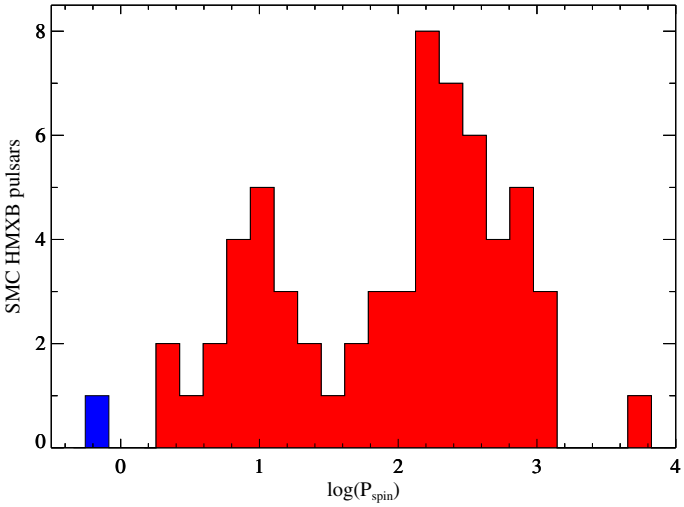

Fig. 7. Spin period histogram for 63 HMXB pulsars in the SMC. BeXRBs are shown in red, while the super-giant system SMC X-1 is depicted in blue.

here that Eger & Haberl (2008a) reported a sharp drop in X-ray luminosity below the detection limit of *XMM-Newton* from SAX J0103.2-7209. The drop occurred after the source reached a level of constant spin period (after years of spin-up) at a luminosity of about 3×10^{35} erg s^{-1} and a small further decrease to 2×10^{35} erg s^{-1}. The authors suggest that this behaviour could be qualitatively explained by the propeller effect, but at a critical luminosity four orders of magnitude higher than expected from Eq. (5) of Stella et al. (1986).

Figure 6 demonstrates that the distributions of the variability factor among BeXRB pulsars and sources without detected pulsations in confidence classes II–V are also similar. If the anti-correlation of variability and spin period also holds for the sources that have no detected spin period (yet), this suggests that most class II–V sources probably have longer spin periods, which would contribute to the long-period peak in the spin-period distribution of Fig. 7. Because sufficiently long observations are required to detect these periods, this could be one reason why they have not yet been found. Conversely, only three (one) class II–V objects have variability factors greater than

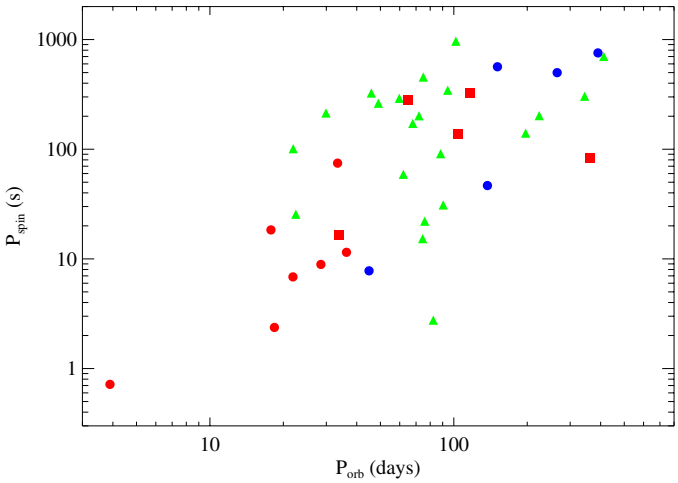

Fig. 8. Spin period vs. orbital period for HMXBs in the SMC. The super-giant HMXB SMC X-1 is found in the lower-left corner. Orbital periods found with different methods are marked with different symbols: orbit solution (red circles), X-ray outbursts (red squares), optical light curve (green triangles). Blue circles mark systems with orbital periods consistently derived from X-rays and optical.

100 (1000). For all three, few X-ray observations exist in general, and none have sufficient statistics to allow a sensitive period search.

In Fig. 7 we present the updated spin period histogram for SMC pulsars, which also includes the two objects with low-significance detections of the period, which need to be confirmed: the 6.878 s detected in Integral data (McBride et al. 2007) and the 154 s period from XMMU J010743.1−715953 (Coe et al. 2012). We also include the long 4693 s period found by Laycock et al. (2010) from a 100 ks *Chandra* observation that may be present in a 23 ks *XMM-Newton* observation (see Sect. 2.2).

Orbital periods of HMXBs and in particular from BeXRBs can be identified from their long-term light curves in X-rays and optical. Long-term monitoring of the SMC pulsars in X-rays was performed by RXTE (Galache et al. 2008), which was sensitive to periodic outbursts near periastron passage of the NS. The OGLE project has monitored stars in the SMC for more than a decade and revealed periodic long-term variability for many Be stars in BeXRBs, which can be attributed to the orbital period of the binary system (Rajoelimanana et al. 2011b). For a few systems the Doppler analysis of the X-ray pulse timing data allowed deriving orbital solutions (e.g. Townsend et al. 2011a). In Fig. 8 we show the spin versus orbital period diagram for the HMXBs in the SMC methodised by different symbols. The first version of such a diagram (Corbet 1984) showed a strong correlation between the two parameters for BeXRBs. Our most recent version contains five times more systems and the correlation has considerably weakened. The correlation is thought to be explained by a quasi-equilibrium state of the neutron star in which the co-rotation radius equals the Alfvén radius. In this picture, the rotation period and the magnetic field strength of the neutron star and the accretion rate determine whether matter can be accreted onto the neutron star (and spin it up) or not (leading to spin-down). The large scatter seen in our updated diagram (the spread in spin period for orbital periods between 50 and 100 days is ~2.5 orders of magnitude) suggests that many of the neutron stars do not rotate near their equilibrium rate, even bearing in mind that the model is too simple.

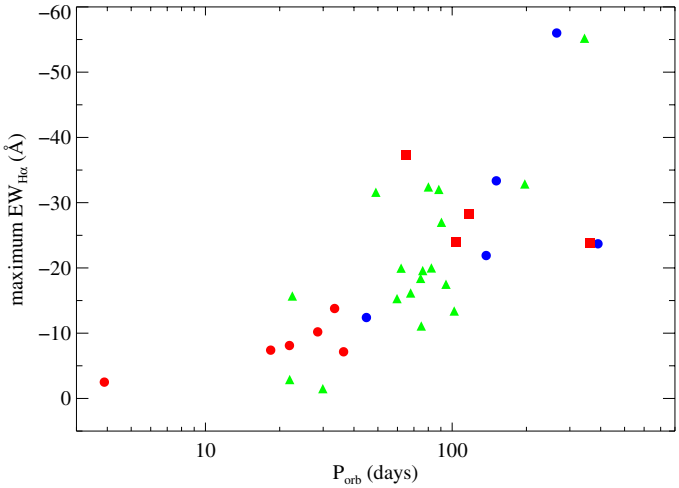

Fig. 9. Equivalent width of the Hα line vs. orbital period for HMXBs in the SMC. The symbols mark the different origin of orbital periods as in Fig. 8. When more than one measurement of the equivalent width is available the largest (most negative) value is used.

In Fig. 9 we present another diagram that is important for characterising the properties of BeXRBs; the equivalent width (observed maximum) is plotted as function of orbital period. For all except one of the objects in this figure, that is, all whose orbital period is known and that have Hα measurements, the spin period is known as well. The exception is the unclear case of RX J0049.2-7311, which we do not associate with SXP9.13 (see Sect. 2.1.1). If the minimum equivalent width is used for objects with more than one Hα measurement, the plot is not significantly altered. Coe & Kirk (2015) investigated the dependence of the equivalent width on orbital period in more detail, in particular with respect to the size of the circum-stellar disc and disc truncation by the compact object (see also Reig et al. 1997). Since in their work SXP9.13 is identified with RX J0049.2-7311, our whole sample from Fig. 9 is covered in their analysis, and we refer to that work for more details.

6. Conclusions

We investigated the properties of 148 (candidate) HMXBs in the SMC and catalogued them. We assigned different levels of confidence at which they are genuine HMXB systems for all catalogue entries. Pulsars are confidence class I, and the probability for being HMXBs decreases until class VI objects. We found many chance coincidences between X-ray and optical position in class VI and rejected 27 candidates as probably misidentified with normal B stars.

The remaining 121 sources comprise a relatively clean sample of HMXBs in the SMC. With 63 pulsars, this indicates that almost 50% of the sources do not have a detected pulse period. A comparison of X-ray variability as function of spin period for pulsars and "non-pulsars" suggests that many long spin periods (longer than a few 100 s) have probably not been found as yet because of the intrinsic short-term X-ray variability of BeXRBs and insufficient observation time. Therefore, it remains unclear how many neutron stars in BeXRBs do not exhibit pulsations because their magnetic field axis is (nearly) aligned with the rotation axis. The larger long-term X-ray variability of objects with short spin period also indicates different accretion schemes for short and long spin period pulsars, which may favour the accretion model of Cheng et al. (2014) to explain the bimodal distribution of spin periods observed from BeXRBs.

Acknowledgements. R.S. acknowledges support from the BMWI/DLR grant FKZ 50 OR 0907 during his stay at MPE.

Note added in proof. A recent observation with *XMM-Newton* has shown that catalogue entries number 2 and 142 belong to the same BeXRB (Haberl et al. 2015).

References

Antoniou, V., Hatzidimitriou, D., Zezas, A., & Reig, P. 2009a, ApJ, 707, 1080
Antoniou, V., Zezas, A., Hatzidimitriou, D., & McDowell, J. C. 2009b, ApJ, 697, 1695
Azzopardi, M., Vigneau, J., & Macquet, M. 1975, A&AS, 22, 285
Bonanos, A. Z., Lennon, D. J., Köhlinger, F., et al. 2010, AJ, 140, 416
Buccheri, R., Bennett, K., Bignami, G. F., et al. 1983, A&A, 128, 245
Buckley, D. A. H., Coe, M. J., Stevens, J. B., et al. 2001, MNRAS, 320, 281
Chakrabarty, D., Levine, A. M., Clark, G. W., & Takeshima, T. 1998a, IAU Circ., 7048, 1
Chakrabarty, D., Takeshima, T., Ozaki, M., Paul, B., & Yokogawa, J. 1998b, IAU Circ., 7062, 1
Cheng, Z.-Q., Shao, Y., & Li, X.-D. 2014, ApJ, 786, 128
Clark, G. W., Remillard, R. A., & Woo, J. W. 1997, ApJ, 474, L111
Clark, J. S., Bartlett, E. S., Coe, M. J., et al. 2013, A&A, 560, A10
Coe, M. J., & Kirk, J. 2015, MNRAS, 452, 969
Coe, M. J., & Orosz, J. A. 2000, MNRAS, 311, 169
Coe, M. J., Haigh, N. J., Laycock, S. G. T., Negueruela, I., & Kaiser, C. R. 2002, MNRAS, 332, 473
Coe, M. J., Edge, W. R. T., Galache, J. L., & McBride, V. A. 2005, MNRAS, 356, 502
Coe, M. J., Schurch, M., McBride, V. A., et al. 2009, MNRAS, 394, 2191
Coe, M. J., Bird, A. J., Buckley, D. A. H., et al. 2010, MNRAS, 406, 2533
Coe, M. J., Bartlett, E. S., Bird, A. J., et al. 2011a, ATel, 3396, 1
Coe, M. J., Haberl, F., Sturm, R., et al. 2011b, MNRAS, 414, 3281
Coe, M. J., Haberl, F., Sturm, R., et al. 2012, MNRAS, 424, 282
Coe, M. J., Bird, A. J., Kennea, J. A., et al. 2013a, ATel, 5662, 1
Coe, M. J., Bird, A. J., McBride, V., Bartlett, E. S., & Haberl, F. 2013b, ATel, 5547, 1
Coe, M. J., Bird, A. J., McBride, V. A., et al. 2014, ATel, 5806, 1
Coe, M. J., Bartlett, E. S., Bird, A. J., et al. 2015, MNRAS, 447, 2387
Corbet, R. H. D. 1984, A&A, 141, 91
Corbet, R., Marshall, F. E., Lochner, J. C., Ozaki, M., & Ueda, Y. 1998, IAU Circ., 6803, 1
Corbet, R., Markwardt, C. B., Marshall, F. E., Laycock, S., & Coe, M. 2002, IAU Circ., 7932, 2
Corbet, R. H. D., Markwardt, C. B., Marshall, F. E., et al. 2003, ATel, 163, 1
Corbet, R. H. D., Coe, M. J., Marshall, F. E., McBride, V. A., & Schurch, M. P. E. 2008, ATel, 1600, 1
Corbet, R. H. D., Bartlett, E. S., Coe, M. J., et al. 2010, ATel, 2813, 1
Covino, S., Negueruela, I., Campana, S., et al. 2001, A&A, 374, 1009
Cowley, A. P., Schmidtke, P. C., McGrath, T. K., et al. 1997, PASP, 109, 21
Eger, P., & Haberl, F. 2008a, A&A, 491, 841
Eger, P., & Haberl, F. 2008b, A&A, 485, 807
Edge, W. R. T., & Coe, M. J. 2003, MNRAS, 338, 428
Edge, W. R. T., Coe, M. J., Corbet, R. H. D., et al. 2003, ATel, 215, 1
Edge, W. R. T., Coe, M. J., Galache, J. L., et al. 2004a, MNRAS, 353, 1286
Edge, W. R. T., Coe, M. J., & McBride, V. A. 2004b, ATel, 217, 1
Esposito, P., Israel, G. L., Sidoli, L., et al. 2013, MNRAS, 433, 3464
Evans, C. J., Howarth, I. D., Irwin, M. J., Burnley, A. W., & Harries, T. J. 2004, MNRAS, 353, 601
Evans, C. J., Lennon, D. J., & Smartt, S. J. 2006, in Stellar Evolution at Low Metallicity: Mass Loss, Explosions, Cosmology, eds. H. J. G. L. M. Lamers, N. Langer, T. Nugis, & K. Annuk, ASP Conf. Ser., 353, 41
Evans, I. N., Primini, F. A., Glotfelty, K. J., et al. 2010, ApJS, 189, 37
Filipović, M. D., Haberl, F., Pietsch, W., & Morgan, D. H. 2000a, A&A, 353, 129
Filipović, M. D., Pietsch, W., & Haberl, F. 2000b, A&A, 361, 823
Galache, J. L., Corbet, R. H. D., Coe, M. J., et al. 2008, ApJS, 177, 189
Gregory, P. C., & Loredo, T. J. 1996, ApJ, 473, 1059
Haberl, F., & Eger, P. 2008, ATel, 1529, 1
Haberl, F., & Pietsch, W. 2004, A&A, 414, 667
Haberl, F., & Pietsch, W. 2005, A&A, 438, 211
Haberl, F., & Sasaki, M. 2000, A&A, 359, 573
Haberl, F., Filipović, M. D., Pietsch, W., & Kahabka, P. 2000, A&AS, 142, 41
Haberl, F., Pietsch, W., Schartel, N., Rodriguez, P., & Corbet, R. H. D. 2004, A&A, 420, L19

Haberl, F., Pietsch, W., & Kahabka, P. 2007, ATel, 1095, 1
Haberl, F., Eger, P., & Pietsch, W. 2008, A&A, 489, 327
Haberl, F., Sturm, R., Filipović, M. D., Pietsch, W., & Crawford, E. J. 2012a, A&A, 537, L1
Haberl, F., Sturm, R., Tsujimoto, M., et al. 2012b, ATel, 4648, 1
Haberl, F., Vasilopoulos, G., Sturm, R., & Maggi, P. 2015, ATel, 8305, 1
Hénault-Brunet, V., Oskinova, L. M., Guerrero, M. A., et al. 2012, MNRAS, 420, L13
Hughes, J. P., & Smith, R. C. 1994, AJ, 107, 1363
Imanishi, K., Yokogawa, J., & Koyama, K. 1998, IAU Circ., 7040, 2
Israel, G. L., Stella, L., Angelini, L., et al. 1997, ApJ, 484, L141
Israel, G. L., Stella, L., Campana, S., et al. 1998, IAU Circ., 6999, 1
Israel, G. L., Stella, L., Covino, S., Campana, S., & Mereghetti, S. 1999, IAU Circ., 7101, 1
Israel, G. L., Campana, S., Covino, S., et al. 2000, ApJ, 531, L131
Israel, G. L., Esposito, P., D'Elia, V., & Sidoli, L. 2013, ATel, 5552, 1
Kahabka, P., & Hilker, M. 2005, A&A, 435, 9
Kahabka, P., & Pietsch, W. 1996, A&A, 312, 919
Kahabka, P., Pietsch, W., Filipović , M. D., & Haberl, F. 1999, A&AS, 136, 81
Keller, S. C., Wood, P. R., & Bessell, M. S. 1999, A&AS, 134, 489
Kennea, J. A. 2011, ATel, 3578, 1
Knigge, C., Coe, M. J., & Podsiadlowski, P. 2011, Nature, 479, 372
Kourniotis, M., Bonanos, A. Z., Soszyński, I., et al. 2014, A&A, 562, A125
Kozłowski, S., & Kochanek, C. S. 2009, ApJ, 701, 508
Lamb, R. C., Prince, T. A., Macomb, D. J., & Finger, M. H. 1999, IAU Circ., 7081, 4
Lamb, R. C., Macomb, D. J., Prince, T. A., & Majid, W. A. 2002, ApJ, 567, L129
Laycock, S., Corbet, R. H. D., Perrodin, D., et al. 2002, A&A, 385, 464
Laycock, S., Corbet, R. H. D., Coe, M. J., et al. 2005, ApJS, 161, 96
Laycock, S., Zezas, A., Hong, J., Drake, J. J., & Antoniou, V. 2010, ApJ, 716, 1217
Liu, Q. Z., van Paradijs, J., & van den Heuvel, E. P. J. 2005, A&A, 442, 1135
Macomb, D. J., Finger, M. H., Harmon, B. A., Lamb, R. C., & Prince, T. A. 1999, ApJ, 518, L99
Macomb, D. J., Fox, D. W., Lamb, R. C., & Prince, T. A. 2003, ApJ, 584, L79
Maggi, P., Sturm, R., Haberl, F., & Vasilopoulos, G. 2013, ATel, 5674, 1
Maggi, P., Sturm, R., Haberl, F., Vasilopoulos, G., & Udalski, A. 2014, ATel, 5778, 1
Majid, W. A., Lamb, R. C., & Macomb, D. J. 2004, ApJ, 609, 133
Maravelias, G., Zezas, A., Antoniou, V., & Hatzidimitriou, D. 2014, MNRAS, 438, 2005
Marshall, F. E., Lochner, J. C., Santangelo, A., et al. 1998, IAU Circ., 6818, 1
Masetti, N., Parisi, P., Palazzi, E., et al. 2010, A&A, 519, A96
Massey, P. 2002, ApJS, 141, 81
McBride, V. A., Coe, M. J., Bird, A. J., et al. 2007, MNRAS, 382, 743
McBride, V. A., Coe, M. J., Negueruela, I., Schurch, M. P. E., & McGowan, K. E. 2008, MNRAS, 388, 1198
McBride, V. A., Bird, A. J., Coe, M. J., et al. 2010, MNRAS, 403, 709
McGowan, K. E., Coe, M. J., Schurch, M., et al. 2007, MNRAS, 376, 759
McGowan, K. E., Coe, M. J., Schurch, M. P. E., et al. 2008a, MNRAS, 384, 821
McGowan, K. E., Coe, M. J., Schurch, M. P. E., et al. 2008b, MNRAS, 383, 330
Meixner, M., Gordon, K. D., Indebetouw, R., et al. 2006, AJ, 132, 2268
Meyssonnier, N., & Azzopardi, M. 1993, A&AS, 102, 451
Murphy, M. T., & Bessell, M. S. 2000, MNRAS, 311, 741
Nazé, Y., Hartwell, J. M., Stevens, I. R., et al. 2003a, ApJ, 586, 983
Nazé, Y., Rauw, G., Manfroid, J., Chu, Y.-H., & Vreux, J.-M. 2003b, A&A, 401, L13
Novara, G., La Palombara, N., Mereghetti, S., et al. 2011, A&A, 532, A153
Raguzova, N. V., & Popov, S. B. 2005, Astron. Astrophys. Trans., 24, 151
Rajoelimanana, A. F., Charles, P. A., & Udalski, A. 2011a, ATel, 3154, 1
Rajoelimanana, A. F., Charles, P. A., & Udalski, A. 2011b, MNRAS, 413, 1600
Reig, P. 2011, Ap&SS, 332, 1
Reig, P., Fabregat, J., & Coe, M. J. 1997, A&A, 322, 193
Reig, P., Larionov, V., Negueruela, I., Arkharov, A. A., & Kudryavtseva, N. A. 2007, A&A, 462, 1081
Rivinius, T., Carciofi, A. C., & Martayan, C. 2013, A&ARv, 21, 69
Santangelo, A., Cusumano, G., Israel, G. L., et al. 1998, IAU Circ., 6818, 1
Sasaki, M., Haberl, F., & Pietsch, W. 2000, A&AS, 147, 75
Sasaki, M., Haberl, F., Keller, S., & Pietsch, W. 2001, A&A, 369, L29
Sasaki, M., Pietsch, W., & Haberl, F. 2003, A&A, 403, 901
Schmidtke, P. C., & Cowley, A. P. 2005, AJ, 130, 2220
Schmidtke, P. C., & Cowley, A. P. 2006, ATel, 716, 1
Schmidtke, P. C., & Cowley, A. P. 2013, ATel, 5556, 1
Schmidtke, P. C., Cowley, A. P., Crane, J. D., et al. 1999, AJ, 117, 927
Schmidtke, P. C., Cowley, A. P., Levenson, L., & Sweet, K. 2004, AJ, 127, 3388
Schmidtke, P. C., Cowley, A. P., & Udalski, A. 2009, ATel, 1953, 1
Schmidtke, P. C., Cowley, A. P., & Udalski, A. 2013a, MNRAS, 431, 252
Schmidtke, P. C., Cowley, A. P., & Udalski, A. 2013b, ATel, 4936, 1
Schmidtke, P. C., Cowley, A. P., & Udalski, A. 2014, ATel, 5776, 1
Schurch, M. P. E., Coe, M. J., McGowan, K. E., et al. 2007, MNRAS, 381, 1561
Schurch, M. P. E., Coe, M. J., McBride, V. A., et al. 2011, MNRAS, 412, 391
Shtykovskiy, P., & Gilfanov, M. 2005, MNRAS, 362, 879
Skrutskie, M. F., Cutri, R. M., Stiening, R., et al. 2006, AJ, 131, 1163
Smith Neubig, M. M., & Bruhweiler, F. C. 1997, AJ, 114, 1951
Stella, L., White, N. E., & Rosner, R. 1986, ApJ, 308, 669
Stevens, J. B., Coe, M. J., & Buckley, D. A. H. 1999, MNRAS, 309, 421
Sturm, R., Pietsch, W., Haberl, F., & Immler, S. 2010, ATel, 2876, 1
Sturm, R., Haberl, F., Coe, M. J., et al. 2011a, A&A, 527, A131
Sturm, R., Haberl, F., Pietsch, W., Immler, S., & Udalski, A. 2011b, ATel, 3575, 1
Sturm, R., Haberl, F., Pietsch, W., & Udalski, A. 2011c, ATel, 3761, 1
Sturm, R., Haberl, F., Pietsch, W., et al. 2012, A&A, 537, A76
Sturm, R., Drašković, D., Filipović, M. D., et al. 2013a, A&A, 558, A101
Sturm, R., Haberl, F., Oskinova, L. M., et al. 2013b, A&A, 556, A139
Sturm, R., Haberl, F., Pietsch, W., et al. 2013c, A&A, 558, A3
Sturm, R., Haberl, F., Pietsch, W., & Udalski, A. 2013d, A&A, 551, A96
Sturm, R., Haberl, F., Vasilopoulos, G., et al. 2014, MNRAS, 444, 3571
Townsend, L. J., Coe, M. J., Corbet, R. H. D., & Hill, A. B. 2011a, MNRAS, 416, 1556
Townsend, L. J., Drave, S. P., Corbet, R. H. D., Coe, M. J., & Bird, A. J. 2011b, ATel, 3311, 1
Tsujimoto, M., Imanishi, K., Yokogawa, J., & Koyama, K. 1999, PASJ, 51, L21
Udalski, A., Szymanski, M., Kubiak, M., et al. 1998, Acta Astron., 48, 147
Wada, Q., Tsujimoto, M., & Ebisawa, K. 2012, ATel, 4628, 1
Wada, Q., Tsujimoto, M., Ebisawa, K., & Miller, E. D. 2013, PASJ, 65, L2
Wyrzykowski, L., Udalski, A., Kubiak, M., et al. 2004, Acta Astron., 54, 1
Yokogawa, J., & Koyama, K. 1998a, IAU Circ., 7009, 3
Yokogawa, J., & Koyama, K. 1998b, IAU Circ., 7028, 1
Yokogawa, J., Imanishi, K., Ueno, M., & Koyama, K. 2000a, PASJ, 52, L73
Yokogawa, J., Torii, K., Imanishi, K., & Koyama, K. 2000b, PASJ, 52, L37
Yokogawa, J., Torii, K., Kohmura, T., Imanishi, K., & Koyama, K. 2000c, PASJ, 52, L53
Yokogawa, J., Imanishi, K., Tsujimoto, M., Koyama, K., & Nishiuchi, M. 2003, PASJ, 55, 161
Zaritsky, D., Harris, J., Thompson, I. B., Grebel, E. K., & Massey, P. 2002, AJ, 123, 855

Appendix A: Additionnal tables

Table A.1. Catalogue of HMXBs and candidates in the SMC.

No	RA	Dec	ERR	O	MA93	*U*	*B*	*V*	*I*	*Q*	*eQ*	*D*	Pspin	ID	Conf. class and flags
1	01 17 05.2	−73 26 36	0.5	N		12.23	13.01	13.15	13.17	−0.67	0.16	0.8	0.717	HMXB supergiant SMC X-1	1 ps oi em os
2	01 19 00.0	−73 12 27	220.0	X	1868	14.27	14.96	15.04				222.7	2.165	HMXB Be/X? XTEJ0119-731 (GCC08), counterpart? Lin 526, opt: M02	1 ps oi: em
3	00 54 30.9	−73 40 55	10.5	R		13.77	14.75	14.73	14.67	−0.99	0.06	12.4	2.370	HMXB Be/X SMC X-2 (no XMM); likely optical counterp. from OGLE-III variability	1 ps px po xv oi em os
4	00 59 11.4	−71 38 45	7.5	R	−179	13.09	14.07	14.01	14.03	−1.02	0.08	6.6	2.763	HMXB Be/X RXJ0059.2-7138; ASCA: 10^{38} erg/s; XMM UL	1 ps po xv xs oi em oo
5	00 52 17.0	−72 19 51	111.0	X									4.780	HMXB Be/X? XTEJ0052-723; [MA93]537 Halpha EQW=−43.3A OR AzV 129 Porb=23.9d	1 ps px po oi: em
6	00 57 02.3	−72 25 55	0.5	C		14.77	15.76	15.96	15.75	−0.85	0.20	0.5	5.050	HMXB Be/X IGR J00569-7226 (CBM13, CBK13, CBB15)	1 ps px: po xv xs oi em
7	01 02 53.4	−72 44 35	0.5	N		13.68	14.79	14.98	15.08	−0.98	0.04	0.1	6.850	HMXB Be/X XTEJ0103-728 = XMMUJ010253.1-724433 (HPK07)	1 ps px po xv xs oi em os
8	00 54 10.0	−72 25 44	204.0	I									6.878	HMXB? Integral 2.6sigma period (MCB07)	1 ps:
9	00 52 05.7	−72 26 04	0.6	C	531	13.94	14.91	14.91	14.83	−0.97	0.05	0.1	7.780	HMXB Be/X SMC X-3 (ECG04)	1 ps px po xv xs oi em oxo
10	00 57 58.4	−72 22 30	1.5	C		14.60	15.64	15.72	15.93	−0.98	0.05	1.2	7.920	HMXB Be/X SXP7.92 = CXOU J005758.4-722229 (CCM08, IED13, SC13)	1 ps po xv xs oi em
11	00 51 53.2	−72 31 48	1.0	C	506	13.66	14.79	14.38	14.40	−1.42	0.11	0.4	8.900	HMXB Be/X RXJ0051.8-7231 (ISA97, SCB99)	1 ps px po oi em os
12	00 49 18.5	−73 12 01	40.0	A									9.130	HMXB Be/X AXJ0049-732 (YIT03, GCC08)	1 ps px xs:
13	01 04 42.3	−72 54 04	0.6	C		13.84	14.89	14.86	15.50	−1.06	0.06	0.8	11.480	HMXB Be/X IGRJ01054-7253 = CXOU J010442.29-725404.4 (HEASARC cxoxassist)	1 ps px po xv xs oi em os
14	01 57 16.0	−72 58 33	3.8	S			14.40	15.00				0.9	11.580	HMXB Be/X? IGR J015712-7259 in Magellanic Bridge; opt. from NOMAD	1 ps px po xv xs oi
15	00 48 14.0	−73 22 04	0.5	N		13.96	14.90	15.02	15.25	−0.85	0.05	0.4	11.866	HMXB Be/X XMMUJ004813.9-732203 (SHC11)	1 ps xv xs oi em
16	00 52 14.0	−73 19 18	1.0	C	552	13.68	14.63	14.49	14.41	−1.06	0.09	0.6	15.300	HMXB Be/X RXJ0052.1-7319 (LPM99, ISC99, HEP08)	1 ps px po oi em oo
17	00 50 44.6	−73 16 05	1800.	X									16.600	HMXB XTEJ0050-731 (LMP02) is NOT RXJ0051.9-7311; coord: 1deg FWHM	1 ps px ox
18	00 49 11.5	−72 49 36	0.5	N		15.22	16.01	15.96	15.89	−0.82	0.04	1.1	18.370	HMXB Be/X XTE J0055-727 = XMMU J004911.4-724939, XMM survey	1 ps px po xs oi os
19	01 17 40.4	−73 30 51	1.3	N	1845	13.30	14.14	14.18	14.09	−0.82	0.06	1.3	22.070	HMXB Be/X RXJ0117.6-7330 (MFH99, CRW97) weak in XMM survey	1 ps xv oi em oo
20	00 48 14.2	−73 10 04	0.6	N		15.06	15.56	15.30	15.51	−0.69	0.06	0.1	25.550	HMXB Be/X XMMU J004814.1-731003 =? RXTE 25.5s or 51s pulsar (LMP02, GCC08)	1 ps xs oi em oo
21	01 11 08.6	−73 16 46	0.7	N		14.40	15.42	15.52	15.29	−0.96	0.05	0.1	31.030	HMXB Be/X XTEJ0111.2-7317 (CLC98, ISC99); in XMM survey (SHP13)	1 ps po oi em oo
22	00 53 55.2	−72 26 46	0.6	C		13.63	14.65	14.72	14.58	−0.97	0.05	0.9	46.630	HMXB Be/X XTEJ0053-724 (CML98), Chandra (MCS08), *Swift* (SPH10)	1 ps px po xv xs oi em oxo
23	00 54 56.3	−72 26 47	0.6	N	810	14.15	15.21	15.27	15.11	−1.03	0.04	0.1	59.070	HMXB Be/X RXJ0054.9-7226=XTEJ0055-724 (MLS98, SCI98, SCB99, SPH03)	1 ps px po oi em oo
24	01 07 12.6	−72 35 34	0.9	C	1619	14.72	15.55	15.64	15.73	−0.77	0.09	0.5	65.780	HMXB Be/X CXOUJ010712.6-723533=2E0105.7-7251=RXJ0107.1-7235=AXJ0107.2-7234 MCS07	1 ps po xs oi em
25	00 49 03.3	−72 50 52	0.6	N		16.02	16.86	16.78	16.61	−0.90	0.06	0.4	74.670	HMXB Be/X AXJ0049-729 (CML98, SCB99, YIT03), XMM survey (SHP13)	1 ps px po xv xs oi em os

Notes. The full version of the catalogue is available at the CDS and regular updates will be posted at http://www.mpe.mpg.de/heg/SMC

Table A.1. continued.

No	RA	Dec	ERR	O	MA93	*U*	*B*	*V*	*I*	*Q*	*eQ*	*D*	Pspin	ID	Conf. class and flags
26	00 52 08.9	−72 38 03	0.6	C		14.33	15.15	15.23	14.83	−0.76	0.05	0.8	82.400	HMXB Be/X XTEJ0052-725 (CMM02, ECC03, GCC08)	1 ps px oi em ox
27	00 50 57.1	−72 13 33	0.5	N	413	14.01	14.99	15.06	14.86	−0.93	0.06	0.7	91.120	HMXB Be/X AXJ0051-722 (CML98, SCB99, CBB11)	1 ps px po xv oi em oo
28	00 53 53.0	−72 26 42	1800.	X									95.000	HMXB XTE SMC95 (LCP02), Porb? (GCC08), position? 1deg FWHM	1 ps
29	00 57 27.1	−73 25 19	0.8	C		14.73	15.62	15.67	15.61	−0.86	0.12	0.4	101.160	HMXB Be/X AXJ0057.4-7325=RXJ0057.3-7325 (YTK00, MCS07), Porb? (GCC08)	1 ps px po xs oi em: oo
30	00 53 24.0	−72 27 16	1.0	C	667	15.06	16.11	16.19	16.14	−0.99	0.09	0.7	138.000	HMXB Be/X CXOU J005323.8-722715 (ECG04, MCN08)	1 ps px po xs oi em ox
31	00 56 05.7	−72 21 59	0.9	N	904	14.75	15.84	15.88	15.98	−1.06	0.04	0.8	140.100	HMXB Be/X XMMUJ005605.2-722200 2E0054.4-7237 (HS00, SPH03, CEG05)	1 ps po oi em oo:
32	00 53 53.0	−72 26 42	1800.	X									144.100	HMXB XTE SMC144s (CMM03, GCC08), position? 1deg FWHM	1 ps
33	00 57 50.3	−72 07 57	1.0	C	1038	14.63	15.64	15.69	15.48	−0.97	0.14	1.0	152.340	HMXB Be/X RX J0057.8-7207 (HS00), CXOU J005750.3-720756 (SPH03, MFL03, CEG05)	1 ps xv xs oi em
34	01 07 43.3	−71 59 54	0.6	N	1640	15.47	15.99	16.27	16.47	−0.32	0.05	0.9	153.990	HMXB Be/X XMMUJ010743.1-715953, XMM survey, Pspin 2sigma (CHS12)	1 ps: xs oi em
35	00 52 55.1	−71 58 06	0.5	N	623	14.37	15.48	15.53	15.34	−1.07	0.06	0.6	169.300	HMXB Be/X RXJ0052.9-7158=XTEJ0054-720=AXJ0052.9-7157=XMMUJ005255.0-715808 CSM97	1 ps px po xv oi em
36	00 51 51.9	−73 10 33	0.9	C	504	13.39	14.38	14.45	14.28	−0.94	0.05	1.2	172.000	HMXB Be/X RXJ0051.9-7311=AXJ0051.6-7311 (SCC99, YTI00) Porb? (SCM11)	1 ps px po xs oi em oo
37	01 01 52.3	−72 23 33	0.5	N	1288	13.84	14.94	14.94	14.85	−1.09	0.20	0.4	175.400	HMXB Be/X RXJ0101.8-7223=AXJ0101.8-7223=XMMUJ010152.4-722336 (HS00, YIT03, TDC11)	1 ps xs oi em
38	00 59 21.0	−72 23 17	0.5	N		13.81	14.96	14.98	15.07	−1.15	0.04	0.5	201.900	HMXB Be/X RXJ0059.3-7223 (KPF99) XMMUJ005921.0-722317 (SPH03, MLM04) Porb?(GCC08)	1 ps px po xs oi oo
39	00 59 28.9	−72 37 04	0.5	N	1147	14.57	15.58	15.53	15.34	−1.04	0.06	0.8	202.520	HMXB Be/X XMMU J005929.0-723703 (HEP08, SCM11), XMM survey (SHP13)	1 ps po xv xs oi em oo
40	00 50 11.1	−73 00 25	0.5	N		14.03	14.99	15.02	15.12	−0.94	0.04	1.1	214.030	HMXB Be/X XMMUJ005011.1-730026 (XMM survey: CHS11), Porb (SCU13)	1 ps po xv xs oi em: oo
41	00 47 23.3	−73 12 28	0.5	N	172	15.14	16.11	16.03	15.99	−1.03	0.06	0.8	263.000	HMXB Be/X RXJ0047.3-7312 (HS00) XMMUJ004723.7-731226 (HP04) (CEG05, SC05)	1 ps po xv xs oi em oo
42	01 32 51.4	−74 25 45	0.4	N			14.90	15.36				0.4	264.520	HMXB Be/X XMMSL1 J013250.6-742544 = *Swift* J0132.5-7425 in Wing/Bridge (SHV14)	1 ps xs oi
43	00 57 49.4	−72 02 36	0.5	N	1036	14.53	15.54	15.65	15.52	−0.92	0.04	1.1	280.400	HMXB Be/X RXJ0057.8-7202=AXJ0058-72.0 (TIY99, HS00, SPH03, CEG05)	1 ps px: po xv xs oi em ox
44	00 58 12.7	−72 30 48	0.5	N		13.91	14.98	14.87	14.62	−1.14	0.07	0.5	291.330	HMXB Be/X RXJ0058.2-7231 (SCC99, SPH03, EC03) = XTEJ0051-727 (HEP08)	1 ps px po xs oi em oo
45	00 50 48.1	−73 18 18	0.9	N	396	14.20	15.19	15.07	15.00	−1.08	0.06	0.3	292.700	HMXB Be/X (SG05), CXOU J005047.9-731817 (LZH10, SHP13, EIS13)	1 ps xv xs oi em
46	01 01 02.8	−72 06 58	1.2	C	1240	14.67	15.71	15.79	15.62	−0.99	0.05	0.7	304.500	HMXB Be/X RXJ0101.0-7206 (KP96, SCB99, MFL03)	1 ps po xv xs oi em oo
47	00 50 44.6	−73 16 05	0.6	C	387	14.46	15.37	15.48	15.31	−0.83	0.06	0.7	323.200	HMXB Be/X RXJ0050.8-7316=AXJ0051-733 (SCC99, CHL02, YIT03, GCC08)	1 ps px xs oi em ox
48	00 52 52.1	−72 17 15	0.6	N		15.83	16.41	16.62	16.82	−0.43	0.05	0.5	325.400	HMXB Be/X XMMU J005252.1-721715 (HEP08) = CXOU J005252.2-721715 (CSC08, LZH10)	1 ps po xs oi oo

Table A.1. continued.

No	RA	Dec	ERR	O	MA93	*U*	*B*	*V*	*I*	*Q*	*eQ*	*D*	Pspin	ID	Conf. class and flags
49	00 54 03.9	−72 26 32	0.6	N		13.82	14.95	14.94	14.79	−1.13	0.07	0.4	341.900	HMXB Be/X XMMU J005403.8-722632 (HEP08) = CXOU J005403.9-722633 (LZH10)	1 ps xs oi
50	01 03 13.9	−72 09 14	0.9	C	1367	13.65	14.78	14.84	14.69	−1.08	0.05	0.6	345.200	HMXB Be/X SAXJ0103.2-7209 (HS94, ISC98, CO00, ICC00) = AX J0103-722 (YK98)	1 ps po xv xs oi em oo
51	01 01 20.7	−72 11 19	0.5	N	1257	14.41	15.36	15.55	15.53	−0.82	0.06	0.4	455.000	HMXB Be/X RXJ0101.3-7211 (SHK01, SCL04, CEG05)	1 ps po xs oi em oo
52	00 54 55.9	−72 45 11	0.5	N	809	14.04	14.97	15.00	14.90	−0.91	0.18	0.3	499.200	HMXB Be/X CXOUJ005455.6-724510 (ECG04) = XMMUJ005455.4-724512 (HPS04) (SC05)	1 ps px po xs oi em oxo
53	01 02 47.5	−72 04 51	0.8	N		14.69	15.74	16.04	16.31	−0.84	0.05	0.5	522.500	HMXB Be/X 2XMM J010247.4-720449 = Suzaku J0102-7204 (SHP11, WTE12, HST12, WTE13)	1 ps xv xs oi em
54	00 57 36.2	−72 19 34	0.7	C	1020	14.95	16.00	15.99	15.80	−1.06	0.21	0.7	565.000	HMXB Be/X CXOUJ005736.2-721934 (MFL03, SPH03, SCL04, CEG05)	1 ps px po xv xs: oi em oxo
55	00 55 35.4	−72 29 07	0.5	N		13.60	14.65	14.69	14.67	−1.02	0.04	1.0	644.600	HMXB Be/X XMMU J005535.2-722906 (HEP08)	1 ps xs oi
56	00 55 18.3	−72 38 52	0.5	N		15.45	15.92	15.77	15.65	−0.58	0.08	1.0	701.600	HMXB Be/X XMMU J005517.9-723853 (HPS04, RCU11), Vmag from ZHT02 wrong	1 ps po: xs oi oo
57	01 05 55.4	−72 03 49	0.5	N	1557	14.50	15.64	15.70	15.57	−1.09	0.39	1.3	726.000	HMXB Be/X RXJ0105.9-7203=AXJ0105.8-7203 (HS00, YIT03, SPH03, EH08)	1 ps xv xs oi em
58	00 49 42.1	−73 23 15	0.5	N	315	14.09	15.00	14.85	14.70	−1.01	0.20	0.4	755.500	HMXB Be/X RXJ0049.7-7323=AXJ0049.5-7323 (YIU00, HS00, EC03, HP04, SCL04)	1 ps px po xv xs oi em oxo
59	00 49 29.7	−73 10 59	0.6	N	300	15.46	16.35	16.15	16.00	−1.03	0.06	0.9	894.000	HMXB Be/X RXJ0049.5-7310 = CXO J004929.7-731058 (HS00, HP04, LZH10)	1 ps po xv xs oi em
60	01 02 06.7	−71 41 16	0.8	C	1301	13.53	14.58	14.37	14.42	−1.19	0.27	0.3	967.000	HMXB Be/X CXOU J010206.6-714115 (MCS07, SCM07, HEP08) Porb? (SCU09)	1 ps po xs oi em oo
61	01 27 46.0	−73 32 56	0.6	C		13.36	14.32	14.36		−0.93		0.1	1062.000	HMXB Be/X CXO J012745.97-733256.5 (HSF12, HOG12, SHO13) opt. from M02	1 ps xs oi em
62	01 03 37.5	−72 01 33	1.1	C	1393	13.47	14.55	14.65	14.69	−1.01	0.04	0.1	1323.000	HMXB Be/X RXJ0103.6-7201 (HS00, HP05, SC06)	1 ps po: xv xs oi em
63	00 54 46.2	−72 25 23	1.0	C	798	14.39	15.50	15.36	15.25	−1.21	0.13	0.8	4693.000	HMXB Be/X CXOU J005446.2-722523 (AHZ09, LZH10) XMMU J005446.3-722523 (SHP13)	1 ps: xv xs oi em
64	00 32 56.2	−73 48 20	12.9	R		16.18	16.72	16.90	16.86	−0.41	0.18	13.5		HMXB Be/X RXJ0032.9-7348 (KP96), 2 Be candidates (SCB99), no XMM coverage	4 oi: em
65	00 42 07.8	−73 45 03	0.7	N		16.19	16.68	16.78	16.90	−0.42	0.10	1.4		HMXB Be/X XMMU J004207.7-734503(gam=0.47-0.96)=?AX J0042.0-7344(0.9-2.9) (SHP13)	2 xs oi
66	00 43 15.9	−73 24 39	1.5	N		15.91	16.68	16.74	16.84	−0.73	0.09	2.7		HMXB unlikely, XMMU J004315.8-732439 (weak source SHP13), no Balmer em. (Met16)	6 oi:
67	00 45 00.2	−73 42 47	1.7	N		15.28	15.58	15.57	15.54	−0.30	0.06	1.5		HMXB? Be/X? XMMU J004500.2-734246 (SHP13)	6 oi:
68	00 45 38.0	−73 13 54	29.4	R		12.16	12.97	13.02	13.02	−0.78	0.02	19.9		HMXB Be/X? RXJ0045.6-7313, [MA93]114 or AzV9? (HS00), no XMM detection (SHP13)	6 oi:
69	00 48 18.7	−73 21 00	0.6	N		15.66	16.43	16.18	15.79	−0.95	0.05	0.2		HMXB rejected, XMMU J004818.6-732059 (SG05, AZH09), QSO (KK09, SHP13, SDF13)	6 xs: oi:
70	00 48 34.1	−73 02 31	0.7	N	238	13.97	14.78	14.78	14.76	−0.81	0.04	0.5		HMXB Be/X RX J0048.5-7302 = XMMU J004834.5-730230 (HS00, SG05, HEP08, KBS14)	2 po xv xs oi em
71	00 48 49.0	−73 16 25	4.4	C	258	13.59	14.50	14.56	14.28	−0.87	0.06	1.8		HMXB? Be/X? weak Chandra source (LHZ10), not in EPG10, source real?	4 oi: em
72	00 48 55.6	−73 49 46	0.6	N		13.95	14.69	14.93	14.94	−0.56	0.06	1.3		HMXB Be/X XMMU J004855.5-734946, bright in XMM survey, gamma=0.8 (SHP13)	2 xs oi:
73	00 49 02.7	−73 27 07	1.6	N		14.74	15.61	15.79	15.97	−0.75	0.06	3.5		HMXB rejected, XMMU J004902.6-732707 (SHP13), no Balmer emission (Met16)	6 oi: nem
74	00 49 13.6	−73 11 38	0.5	N		15.71	16.63	16.44	16.28	−1.06	0.06	0.3		HMXB Be/X RXJ0049.2-7311 (FPH00, SG05, CEG05, HEP08, RCU11) =?SXP9.13=AXJ0049-732	2 xs oi em oo

Table A.1. continued.

No	RA	Dec	ERR	O	MA93	*U*	*B*	*V*	*I*	*Q*	*eQ*	*D*	Pspin	ID	Conf. class and flags
75	00 49 22.2	−73 20 06	3.4	C		16.08	16.71	16.62	16.85	−0.70	0.07	1.7		HMXB? weak Chandra source, blue early-type star (LZH10), not in EPG10, real?	6 oi:
76	00 49 30.6	−73 31 09	0.6	N	302	13.73	14.60	14.64	14.55	−0.83	0.06	0.4		HMXB Be/X RX J0049.5-7331 = XMMU J004930.6-733109 (HS00, HEP08, SHP13)	2 xs oi em
77	00 49 41.7	−72 48 43	0.6	C		15.06	16.24	15.99	15.62	−1.35	0.15	0.7		HMXB? CXOU J004941.43-724843.8 (AZH09, MZA13), not in EPG10, source real?	6 oi: em:
78	00 50 04.4	−73 14 26	1.6	C		14.72	15.56	15.50	15.72	−0.88	0.06	0.9		HMXB? weak Chandra source, blue early-type star (LZH10), not in EPG10, real?	6 oi:
79	00 50 12.2	−73 11 56	1.7	C	341	14.56	15.47	15.31	14.98	−1.02	0.09	1.2		HMXB? Be/X? weak Chandra source (LZH10)	4 oi: em
80	00 50 35.5	−73 14 01	1.1	C		15.21	16.10	15.99	15.99	−0.97	0.05	1.5		HMXB? weak Chandra source, blue early-type star (LZH10)	6 oi:
81	00 50 36.0	−73 17 39	0.9	C	374	14.72	15.69	15.61	15.40	−1.03	0.05	0.8		HMXB? Be/X? weak Chandra source (LZH10)	4 oi: em
82	00 50 46.9	−73 32 48	33.7	R		14.96	15.64	15.61	15.42	−0.70	0.06	9.9		HMXB? Be/X? RX J0050.7-7332 [MA93]393? (HS00) XMM source 11arcsec away AGN?	6 oi:
83	00 50 47.8	−73 17 36	1.0	C		15.65	16.58	16.58	16.47	−0.94	0.05	0.5		HMXB? weak Chandra source, blue early-type star (LZH10)	6 oi:
84	00 50 57.3	−73 10 08	0.5	N	414	13.55	14.43	14.35	14.40	−0.94	0.06	0.6		HMXB Be/X RXJ0050.9-7310 = CXO J005057.2-731008 (HS00, SG05, LZH10, SHP13)	2 xs oi em
85	00 51 05.7	−73 13 12	1.2	C		14.84	15.77	15.70	15.52	−0.99	0.06	0.7		HMXB? weak Chandra source, blue early-type star (LZH10)	5 oi
86	00 51 17.0	−73 16 06	1.0	C	448	14.13	15.19	15.00	14.92	−1.19	0.05	0.9		HMXB? Be/X? weak Chandra source (LZH10)	4 oi: em
87	00 51 19.6	−72 50 44	15.6	R		15.45	16.36	16.31	16.01	−0.95	0.05	14.6		HMXB? Be/X? RXJ0051.3-7250 [MA93]447? (HS00) XMM source 17.7arcsec away, AGN?	6 oi:
88	00 51 33.3	−73 30 12	1.5	N		15.85	16.65	16.58	16.72	−0.85	0.32	4.4		HMXB rejected, XMMU J005133.2-733012 (SHP13), no Balmer emission (Met16)	6 oi: nem
89	00 51 46.1	−73 07 04	1.1	N		16.05	16.71	16.73	16.90	−0.64	0.05	2.9		HMXB rejected, XMMU J005146.1-730704 (SHP13), no Balmer emission (Met16)	6 oi: nem
90	00 51 54.2	−72 55 36	40.0	E		14.43	15.49	15.40	15.26	−1.13	0.08	28.2		HMXB Be/X? RXJ0051.9-7255 [MA93]521? (HS00) no XMM detection	6 oi:
91	00 51 59.6	−73 29 26	3.0	S		14.41	15.23	15.18	14.98	−0.85	0.06	4.7		HMXB Be/X IGR J00515-7328 (CBB10, SHP11, K11)	2 xv oi:
92	00 52 07.8	−72 21 26	2.0	N		14.50	15.12	15.20	14.73	−0.57	0.04	1.4		HMXB Be/X? XMMU J005207.8-722125 (LZH10, SHP13, unclassified in AZH09); SXP4.78?	6 oi:
93	00 52 15.4	−73 19 15	1.0	C		14.81	15.76	15.90	16.10	−0.85	0.05	0.4		HMXB Be/X? CXOUJ005215.4-731915 very close to SXP15.3 (LZH10, SHP13)	2 xs oi
94	00 52 35.3	−72 25 21	1.6	N		13.81	14.73	14.90	15.14	−0.80	0.04	5.7		HMXB rejected, XMMU J005235.2-722520 (SHP13), Chandra position incompatible	6 oi:
95	00 52 37.3	−72 27 32	1.2	C	590	13.88	14.99	14.98	14.76	−1.12	0.04	0.4		HMXB? Be/X? weak Chandra source (LZH10)	4 oi: em
96	00 52 45.0	−72 28 44	1.0	C		13.95	14.92	14.92	14.87	−0.97	0.07	0.4		HMXB Be/X CXOUJ005245.0-722844 (LZH10)	3 oi em
97	00 52 52.2	−72 48 30	1.0	C	618	13.35	14.32	14.36	14.24	−0.93	0.05	0.6		HMXB? peculiar CXOU J005252.2-724830 =?2E0051.1-7304 AzV138 (AZH09)	3 oi em
98	00 52 59.5	−72 54 02	2.1	N		16.52	16.98	16.79	16.43	−0.60	0.09	1.6		HMXB? Be/X? XMMU J005259.4-725402; weak source in XMM survey (SHP13)	6 oi:
99	00 53 14.8	−72 18 48	1.7	N		16.99	17.00	16.39	15.53	−0.45	0.05	2.7		HMXB rejected, weak source, Chandra position incompatible (LZH10, SHP13)	6 oi:
100	00 53 18.5	−72 16 18	1.6	N		15.62	16.42	16.58		−0.68	0.05	2.3		HMXB? Be/X? XMMU J005318.5-721617 (SHP13)	6 oi:
101	00 53 29.2	−72 33 48	2.7	C	677	13.69	14.63	14.62	14.57	−0.95	0.29	0.7		HMXB? Be/X? weak Chandra source (LZH10)	4 oi: em
102	00 53 31.8	−72 18 45	5.2	C		15.08	15.86	16.03	16.25	−0.65	0.05	5.4		HMXB unlikely, weak Chandra source (LZH10), not in EPG10, source real?	6 oi: nem

Table A.1. continued.

No	RA	Dec	ERR	O	MA93	*U*	*B*	*V*	*I*	*Q*	*eQ*	*D*	Pspin	ID	Conf. class and flags
103	00 53 34.6	−72 08 42	0.9	N		15.87	16.19	16.19	16.16	−0.31	0.12	2.7		HMXB unlikely, XMMU J005334.6-720842 (SHP13)	6 oi: nem
104	00 53 41.8	−72 53 10	0.8	N		13.66	14.74	14.66	14.49	−1.14	0.19	2.2		HMXB Be/X XMMU J005341.7-725310 (SHP13)	2 xv oi:
105	00 53 52.5	−72 26 39	0.9	C	717	13.52	13.92	13.67	13.13	−0.58	0.12	1.3		HMXB Be/X CXOU J005352.5-722639 close to SXP46.6 (LZH10)	3 oi em
106	00 54 08.7	−72 32 08	1.4	N		16.59	16.86	16.93	16.96	−0.22	0.06	1.1		HMXB? Be/X? weak source detected by Chandra and XMM (LZH10, SHP13)	6 oi:
107	00 54 09.3	−72 41 43	1.4	N	739	13.10	13.77	13.82	12.62	−0.64	0.15	1.3		HMXB rejected, XMMU J005409.2-724143 (SHP13, AZH09), sgB0[e] S18 (CBC13, MZA14)	3 oi em
108	00 54 19.2	−72 20 49	5.8	C		16.04	16.92	16.97	17.20	−0.84	0.08	1.9		HMXB unlikely, weak Chandra source (LHZ10), not in EPG10, source real?	6 oi: nem
109	00 54 26.0	−71 58 24	0.9	N		15.61	16.42	16.56	16.77	−0.71	0.08	2.4		HMXB rejected, XMMU J005425.9-715824 (SHP13), no Balmer emission (Met16)	6 oi: nem
110	00 55 07.3	−72 08 26	1.7	N		16.05	16.77	16.87	16.94	−0.66	0.19	3.9		HMXB unlikely, XMMU J005507.2-720825 (SHP13)	6 oi: nem
111	00 55 07.7	−72 22 40	0.9	N		13.23	14.26	14.38	14.58	−0.93	0.06	0.8		HMXB Be/X? XMMU J005507.7-722240 = CXOU J005507.7-722241 (SHP13, LZH10)	5 oi
112	00 55 35.0	−71 33 41	1.3	N		15.10	15.94	16.08	16.37	−0.74	0.05	4.7		HMXB rejected, XMMU J005535.0-713340 (SHP13), no Balmer emission (Met16)	6 oi: nem
113	00 55 49.8	−72 51 27	1.5	N		15.86	16.48	16.49	16.65	−0.62	0.06	1.0		HMXB rejected, (SHP13), OGLEII eclipsing binary (WUK04)	6 oi: nem
114	00 56 05.5	−72 00 11	2.0	N		15.69	16.60	16.72	16.97	−0.84	0.05	1.3		HMXB Be/X XMMU J005605.8-720012 (NLM11, SHP13)	3 oi em
115	00 56 13.9	−72 30 00	1.0	N		13.49	14.53	14.52	14.39	−1.05	0.04	0.7		HMXB Be/X XMMU J005613.8-722959 (SHP13)	3 oi em
116	00 56 14.6	−72 37 56	0.8	N	922	13.43	14.71	14.58	14.21	−1.37	0.34	0.7		HMXB Be/X XMMU J005614.6-723755 (SHP13)	3 oi em
117	00 56 18.9	−72 28 03	0.7	N		14.58	14.93	15.32	15.56	−0.07	0.35	3.1		HMXB? Be/X? XMMU J005618.8-722802, Be star: NGC 330:KWBBe 224 (KWB99, SG05, SHP13)	4 xs: oi: em
118	00 56 19.0	−72 15 06	1.8	N		15.18	16.06	16.13	16.12	−0.84	0.06	5.2		HMXB rejected, XMMU J005619.0-721506 (SHP13), Chandra position incompatible	6 oi:
119	00 57 23.7	−72 23 56	0.8	N		13.60	14.64	14.71	14.92	−0.98	0.05	1.7		HMXB Be/X? XMMU J005723.4-722356 (SG05, SHP13, MZA14) rel. large dist to ZHT02	2 xv oi: em:
120	00 57 59.5	−71 56 37	19.2	R		14.36	14.98	14.94	14.84	−0.65	0.20	21.0		HMXB Be/X? RXJ0057.9-7156 [MA93]1044? (HS00) no XMM detection	6 oi:
121	01 00 30.3	−72 20 33	1.0	N	1208	13.57	14.59	14.64	14.54	−0.98	0.17	0.7		HMXB Be/X XMMUJ010030.2-722035 (SPH03, SG05)	3 oi em
122	01 00 37.3	−72 13 17	0.9	N		15.59	16.51	16.68	16.83	−0.80	0.05	2.4		HMXB rejected, XMMU J010037.3-721317 (SG05), AGN? (SHP13), no Balmer em. (Met16)	6 oi:
123	01 00 55.8	−72 23 20	1.0	N			15.49	15.61				1.1		HMXB? Be/X? (SHP13), Bmag from ZHT02 wrong, using B-V from M02	3 oi em
124	01 01 47.6	−71 55 51	0.9	N	1284	13.26	14.40	14.47	14.30	−1.09	0.05	1.4		HMXB SSS Be/WD? XMMUJ010147.5-715550 (SHP12)	3 oi em
125	01 01 55.8	−72 32 37	0.6	N		12.72	13.93	14.02	14.01	−1.14	0.10	0.8		HMXB Be/X, wrong ID with SXP7.92 (CSM09), counterpart AzV285 (SHP13), (RCU11)	2 po xv xs oi oo
126	01 01 55.9	−72 10 28	0.9	N		13.93	14.85	15.06	15.31	−0.77	0.40	0.9		HMXB unlikely, XMMU J010155.8-721027 (SHP13), no Balmer emission (Met16)	5 oi
127	01 03 28.5	−72 06 51	0.6	N		15.46	16.32	16.47	16.78	−0.75	0.06	1.9		HMXB rejected, (SG05, SHP13), OGLEII eclipsing binary (WUK04)	6 oi: nem
128	01 03 31.7	−73 01 44	1.0	N		14.09	15.17	15.41	15.65	−0.91	0.04	1.5		HMXB unlikely, XMMU J010331.7-730144 (SHP13), no Balmer emission (Met16)	6 oi:
129	01 03 33.6	−72 04 17	1.6	N		14.98	15.97	16.08	16.38	−0.91	0.10	4.9		HMXB rejected, XMMU J010333.6-720417 (SHP13), Chandra position incompatible	6 oi: nem

Table A.1. continued.

No	RA	Dec	ERR	O	MA93	*U*	*B*	*V*	*I*	*Q*	*eQ*	*D*	Pspin	ID	Conf. class and flags
130	01 03 38.0	−72 02 15	1.6	N		15.32	16.12	16.31	16.52	−0.67	0.07	4.5		HMXB rejected, XMMU J010338.0-720215 (SHP13), Chandra position incompatible	6 oi: nem
131	01 03 55.1	−72 49 53	1.5	N		16.33	16.96	16.25		−1.15	0.18	3.7		HMXB? Be/X? XMMU J010355.0-724952, in NGC376 (SHP13)	6 oi:
132	01 04 29.4	−72 31 37	1.3	N		14.53	15.61	15.79	16.02	−0.96	0.08	1.4		HMXB Be/X XMMU J010429.4-723136 (SHP13, MSH13)	2 po: xv xs: oi
133	01 04 35.5	−72 21 47	0.8	N	1470	14.07	15.18	15.13	14.98	−1.15	0.04	0.6		HMXB Be/X RX J0104.5-7221 = XMMU J010435.4-722147 (HS00, SHP13)	2 xs oi em
134	01 04 48.5	−71 45 42	1.5	N		17.10	17.30	16.87	16.24	−0.51	0.06	4.3		HMXB unlikely, XMMU J010448.5-714541 (SHP13), no Balmer emission (Met16)	6 oi:
135	01 06 00.8	−72 33 04	1.9	N		15.24	16.18	16.27	16.47	−0.88	0.04	2.0		HMXB unlikely, XMMU J010600.7-723303; weak source in XMM survey (SHP13)	6 oi: nem
136	01 06 33.0	−73 15 43	0.6	N	1592	13.78	14.68	15.06	15.07	−0.63	0.06	0.4		HMXB Be/X XMMU J010633.1-731543 (CHS12)	2 xs oi em
137	01 07 44.5	−72 27 42	0.6	C	1641	14.26	15.47	15.49	15.31	−1.21	0.04	1.5		HMXB Be/X CXOU J010744.51-722741.7 = *Swift* J010745.0-722740 (MSH14)	2 xv oi em
138	01 08 20.2	−72 13 47	0.7	N		13.83	14.55	14.67	14.77	−0.62	0.23	2.2		HMXB rejected, XMM (SHP13), Chandra (EPG10), no Balmer em. (Met16), AGN?	6 oi:
139	01 15 03.5	−73 28 19	1.0	N		15.60	16.34	16.48	16.69	−0.65	0.07	1.6		HMXB unlikely, (XMM survey) HR3/4 just outside of HMXB criteria of SHP13	6 oi: nem
140	01 19 03.5	−73 12 21	1.5	N		15.18	15.93	16.04	16.14	−0.68	0.06	5.6		HMXB unlikely, only 1 of 2 detections compatible with B-star (SHP13); SXP2.16?	6 oi: nem
141	01 19 38.9	−73 30 11	0.7	N	1867	14.95	15.78	15.85	15.61	−0.79	0.12	0.3		HMXB Be/X? RX J0119.6-7330 (HS00, SG05, SHP13)	3 xs: oi em
142	01 21 41.0	−72 57 33	4.0	S	1888	13.17	14.23	14.28				3.2		HMXB Be/X IGR J01217-7257 (CBM14) opt. from M02	3 po oi em
143	01 23 27.5	−73 21 23	1.1	N		14.48	15.39	15.45		−0.87		1.4		HMXB Be/X RX J0123.4-7321=XMM J012327.4-732123 (SHP13, SHPU13); opt. from M02	2 po xv xs: oi
144	02 04 49.0	−73 15 27	108.0	I										HMXB? Be/X? IGR J02048-7315, Magellanic Bridge (MBC10)	6
145	02 06 45.7	−74 27 46	4.0	S			14.44	14.77				2.5		HMXB Be/X? *Swift* J0208.4-7428, Magellanic Bridge (MBC10, SCU14), opt. from NOMAD	2 xv xs oi em
146	02 09 37.2	−74 27 12	30.0	R			14.16	14.53				10.7		HMXB Be/X RXJ0209.6-7427 Mag. Bridge, var 20 in PSPC lc (KH05), opt. from NOMAD	2 xv xs oi em
147	02 22 01.0	−75 57 59	108.0	I										HMXB? Be/X? IGR J02220-7558, Magellanic Bridge (MBC10)	6
148	03 14 23.0	−74 04 23	300.0	I										HMXB? Be/X? IGR J03144-7404, Magellanic Bridge (MBC10)	6

Table A.2. Key references.

Code[a]	Reference	Code[a]	Reference
AHZ09	Antoniou et al. (2009a)	AZH09	Antoniou et al. (2009b)
BCS01	Buckley et al. (2001)	BLK10	Bonanos et al. (2010)
CBB10	Coe et al. (2010)	CBB11	Coe et al. (2011a)
CBB15	Coe et al. (2015)	CBC13	Clark et al. (2013)
CBK13	Coe et al. (2013a)	CBM13	Coe et al. (2013b)
CBM14	Coe et al. (2014)	CCM08	Corbet et al. (2008)
CEG05	Coe et al. (2005)	CHL02	Coe et al. (2002)
CHS11	Coe et al. (2011b)	CHS12	Coe et al. (2012)
CLC98	Chakrabarty et al. (1998a)	CML98	Corbet et al. (1998)
CMM02	Corbet et al. (2002)	CMM03	Corbet et al. (2003)
CNC01	Covino et al. (2001)	CO00	Coe & Orosz (2000)
CRW97	Clark et al. (1997)	CSC08	Schmidtke et al. (1999)
CSM97	Cowley et al. (1997)	CSM09	Coe et al. (2009)
CTO98	Chakrabarty et al. (1998b)	EC03	Edge & Coe (2003)
ECC03	Edge et al. (2003)	ECG04	Edge et al. (2004a)
EH08	Eger & Haberl (2008b)	EHI04	Evans et al. (2004)
EIS13	Esposito et al. (2013)	ELS06	Evans et al. (2006)
EPG10	Evans et al. (2010)	FPH00	Filipović et al. (2000b)
GCC08	Galache et al. (2008)	HEP08	Haberl et al. (2008)
HPK07	Haberl et al. (2007)	HP05	Haberl & Pietsch (2005)
HPS04	Haberl et al. (2004)	HOG12	Hénault-Brunet et al. (2012)
HP04	Haberl & Pietsch (2004)	HS94	Hughes & Smith (1994)
HS00	Haberl & Sasaki (2000)	HSF12	Haberl et al. (2012a)
HST12	Haberl et al. (2012b)	ICC00	Israel et al. (2000)
IED13	Israel et al. (2013)	ISA97	Israel et al. (1997)
ISC98	Israel et al. (1998)	ISC99	Israel et al. (1999)
K11	Kennea (2011)	KBS14	Kourniotis et al. (2014)
KH05	Kahabka & Hilker (2005)	KPF99	Kahabka et al. (1999)
KWB99	Keller et al. (1999)	LCP02	Laycock et al. (2002)
LMP02	Lamb et al. (2002)	LPM99	Lamb et al. (1999)
LZH10	Laycock et al. (2010)	MA93	Meyssonnier & Azzopardi (1993)
M02	Massey (2002)	MBC10	McBride et al. (2010)
MCB07	McBride et al. (2007)	MCN08	McBride et al. (2008)
MCS07	McGowan et al. (2007)	MCS08	McGowan et al. (2008a)
Met16	McBride et al. (in prep.)	MFH99	Macomb et al. (1999)
MFL03	Macomb et al. (2003)	MLM04	Majid et al. (2004)
MLS98	Marshall et al. (1998)	MPP10	Masetti et al. (2010)
MSH13	Maggi et al. (2013)	MSH14	Maggi et al. (2014)
MZA14	Maravelias et al. (2014)	NLM11	Novara et al. (2011)
NHS03	Nazé et al. (2003a)	RCU11	Rajoelimanana et al. (2011b)
SC05	Schmidtke & Cowley (2005)	SC06	Schmidtke & Cowley (2006)
SC13	Schmidtke & Cowley (2013)	SCB99	Stevens et al. (1999)
SCC99	Schmidtke et al. (1999)	SCI98	Santangelo et al. (1998)
SCL04	Schmidtke et al. (2004)	SCM07	Schurch et al. (2007)
SCM11	Schurch et al. (2011)	SCU09	Schmidtke et al. (2009)
SCU13	Schmidtke et al. (2013b)	SCU14	Schmidtke et al. (2014)
SDF13	Sturm et al. (2013a)	SG05	Shtykovskiy & Gilfanov (2005)
SHC11	Sturm et al. (2011a)	SHK01	Sasaki et al. (2001)
SHO13	Sturm et al. (2013b)	SHP11	Sturm et al. (2011c)
SHP12	Sturm et al. (2012)	SHP13	Sturm et al. (2013c)
SHPU13	Sturm et al. (2013d)	SHV14	Sturm et al. (2014)
SPH03	Sasaki et al. (2003)	SPH10	Sturm et al. (2010)
SHP11	Sturm et al. (2011b)	TDC11	Townsend et al. (2011b)
TIY99	Tsujimoto et al. (1999)	WTE12	Wada et al. (2012)
WTE13	Wada et al. (2013)	WUK04	Wyrzykowski et al. (2004)
YIT03	Yokogawa et al. (2003)	YIU00	Yokogawa et al. (2000a)
YK98	Yokogawa & Koyama (1998a)	YTI00	Yokogawa et al. (2000b)
YTK00	Yokogawa et al. (2000c)	ZHT02	Zaritsky et al. (2002)

Notes. [(a)] As used in the comment column of Table A.1.